Contents lists available at SciVerse ScienceDirect

CIRP Annals Manufacturing Technology

Journal homepage: www.elsevier.com/locate/cirp

# Broaching: cutting tools and machine tools for manufacturing high quality features in components

Pedro J. Arrazola [a] (1), Joël Rech [b] (2), Rachid M'Saoubi [c] (1) Dragos Axinte [d, e] (1)

*a Faculty of Engineering, Mondragon University, Mondragón 20500, Spain*
*b University of Lyon, ENISE, CNRS LTDS UMR5513, 42000 Saint-Etienne, France*
*c R&D Materials and Technology Development, Seco Tools AB, SE-73782 Fagersta, Sweden*
*d Machining and Condition Monitoring Group, Faculty of Engineering, University of Nottingham, Nottingham NG7 2RD, United Kingdom*
*e Faculty of Science and Engineering, University of Nottingham Ningbo, Ningbo, China*
*Corresponding author: Pedro J. Arrazola Tel.: +34 943 73 96 64; fax: +34 943 79 15 36.*
*E-mail address: pjarrazola@mondragon.edu*

Broaching is a unique machining process with high accuracy and surface quality, which is employed in mass and batch production for the manufacture of components with highly complex geometries. It involves the use of multiple-edged complex tools in which the cutting edges are arranged with an offset also known as "rise per tooth" that determines the depth of cut per tooth. This paper presents the state-of-the-art of both the experimental and modelling aspects of broaching, and identifies the most important features related to this machining process. This includes a critical assessment of specifically designed broaching setups and their applicability and/or limitations compared to the machines used in industry. Contributions from academia and industry are included to support a comprehensive report of recent advances, as well as a roadmap for future developments.

Broaching, Machining, Modelling, Chip formation

## 1. Introduction

### *1.1 History*

Broaching is a machining process that originated the 1860s in the United States and was initially used for the production of pulley grooves and gears. The first broaching operations were carried out manually; the operator pushed the broaching tool into the hole by repeatedly applying hammer strikes to the tool.

The term broaching appeared for the first time in 1873 and was patented by Anson P. Stephens, who went on to develop the first broaching machine [91] (see Figure 1).

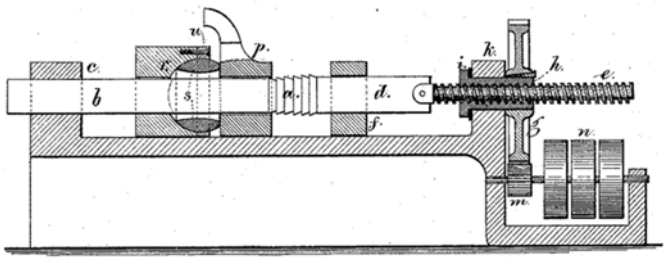

***Figure 1.*** *Broaching machine patented by Stephens in 1873* [91].

Between 1898 and 1902, the Canadian Francis J. Lapointe used this process for the first time in an industrial context, in the form of a horizontal stapler driven by a screw mechanism. He patented this version in 1914 [58], improved it in 1920 [59] and in 1921, the company Oilgear Co. started selling the first hydraulic puller.

The standard DIN 8589-5 classifies the broaching process and tools as set out in Figure 2.

Some examples of holes made by broaching are shown in Figure 3c.

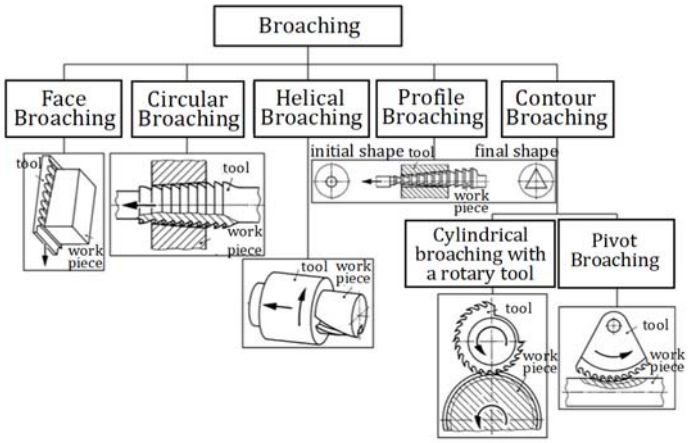


***Figure 2.*** *Classification of broaching process and tools ( DIN-8589-5).*

### *1.2 Broaching process basics*

Broaching is a material removal process where a special tool called a broach (or broaching tool), generally with a linear movement, removes the material in a progressive way.

The main characteristic of a broach is a longitudinal series of teeth arranged geometrically on a shaft or a plate. The dimensions of the teeth increase with the length of the tool, and the rise per tooth, together with other machining conditions, determines the chip thickness.

It is estimated that broaching represents 2-4% of all machining operations. This is a significant figure considering that 15% of the products in the world are manufactured by machining.

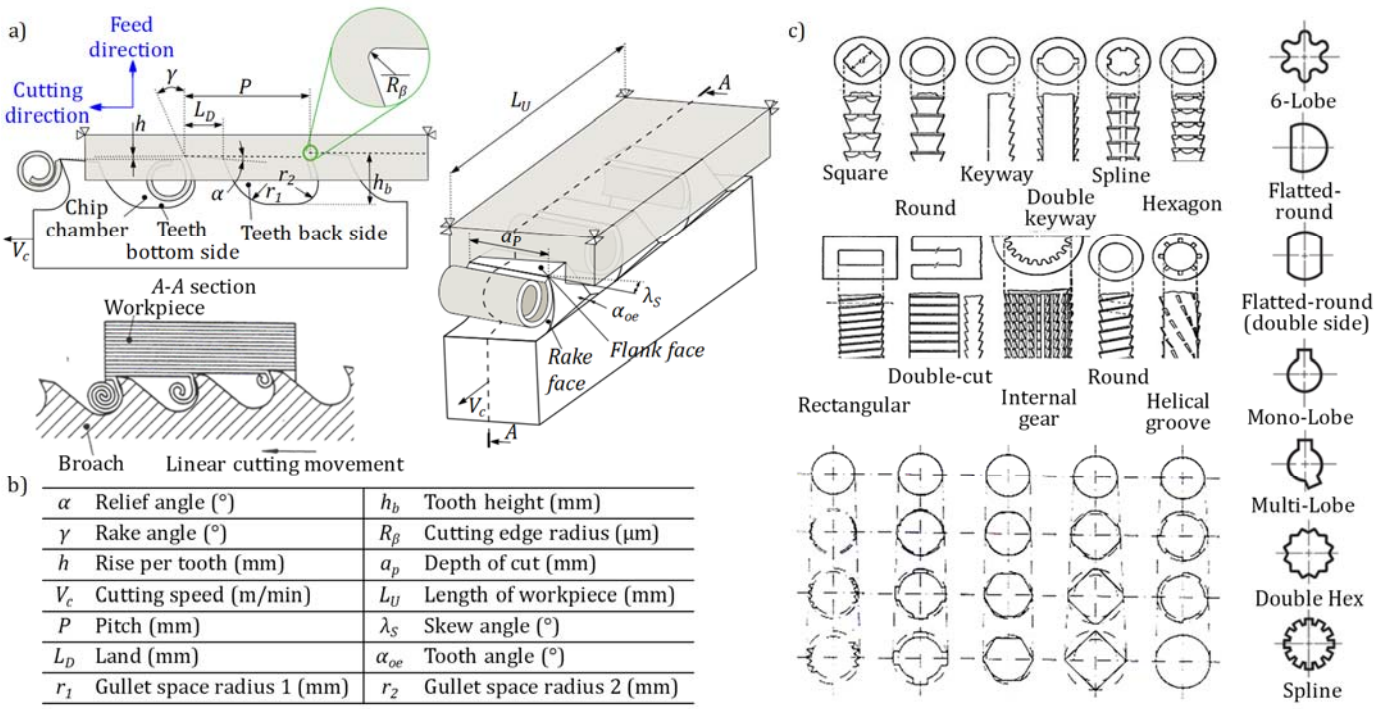


b)

| | | | |
|---|---|---|---|
| $\alpha$ | Relief angle (°) | $h_b$ | Tooth height (mm) |
| $\gamma$ | Rake angle (°) | $R_\beta$ | Cutting edge radius (μm) |
| $h$ | Rise per tooth (mm) | $a_p$ | Depth of cut (mm) |
| $V_c$ | Cutting speed (m/min) | $L_U$ | Length of workpiece (mm) |
| $P$ | Pitch (mm) | $\lambda_S$ | Skew angle (°) |
| $L_D$ | Land (mm) | $\alpha_{oe}$ | Tooth angle (°) |
| $r_1$ | Gullet space radius 1 (mm) | $r_2$ | Gullet space radius 2 (mm) |

***Figure 3.*** *(a) Description of basic principles and tool specifications for a broaching operation* [27]. *(b) Nomenclature of broaching process variables. (c) Different workpiece profiles and corresponding broaching tool geometries.*

Broaching tools cut in a linear motion in one direction only. This movement can be produced by traction or thrust. The machined depth in one pass is achieved by the progressive increase in the dimensions (e.g., height) of the teeth of the broaching tool (see Figure 3a). If the thickness of the material to be removed is significant, or if the machine has force limitations, it may be necessary to manufacture a set of broaching tools/segments that can be mounted one after the other on the machine ram.

Broaching is most commonly an internal process where the tool operates within a hole (where radial forces compensate), but it can also be external if the tool is applied to an open surface.

The field of application is for components that have some geometric complexity, and require a high degree of dimensional accuracy (IT6/IT7), good surface finish ($Ra$ = 0.8μm), as well as high repeatability.

One of the main differences between conventional methods of machining (e.g., milling, turning) and broaching is the speed at which the material is removed. Typical cutting speeds for broaching are between 2.5 and 80 m·min$^{-1}$ compared to values of 75-450 m·min$^{-1}$ for conventional processes.

While the initial investment costs (i.e., machine: €300,000-€1,000,000) and consumables (i.e., broaching tools: €1,000-6,000) may seem high, when considered in the context of large volume production (where the process is usually employed), the cost per part is reduced considerably compared to batch production.

Thus, broaching could be considered among the most effective methods to mass produce parts given its low cost per part, and for this reason it is frequently employed by manufacturers for the automotive, aeronautical and power generation sectors. In the automotive sector, components such as brake caliper brackets, ring gears of epicyclic gear trains and gear box synchronizer rings are manufactured by broaching. In the aeronautic sector, broaching is used to produce components from aeroengines such as dovetails in compressor discs and fir tree roots in turbine discs. In the case of the energy sector, tube sheets in cooling systems (trefoil or quatrefoil shaped holes) of nuclear power plants are manufactured using the broaching process. Figure 4 shows examples of these applications.

### *1.3 Paper objectives and outline*

The main goal of this work is to summarize and critically analyse recent significant developments in broaching science and technology. The article traces advances in broaching since the beginnings of the process, highlights the fundamentals of controlling the process outputs (e.g., part accuracy, surface integrity, tool wear, process stability), and considers future perspectives. Various research groups have made significant progress in broaching in the last 40 years, and these achievements are summarized in eleven major sections. Section 2 outlines process fundamentals by focusing on the mechanisms of chip formation. Section 3 is dedicated to materials, coatings, and broaching tool design. Section 4 provides an overview of the fixture systems for clamping the components to be broached. In Section 5, the type of machine tools employed in broaching is discussed. Section 6 considers the implications of applying process monitoring to broaching, while Section 7 reviews modelling of broaching processes. Some examples of industrial applications are presented in Section 8, demonstrating the real potential of the process. The article closes by presenting alternative solutions to broaching in Section 9, exploring future trends in Section 10, highlighting implications for academia in Section 11, and finishes with concluding remarks in Section 12.

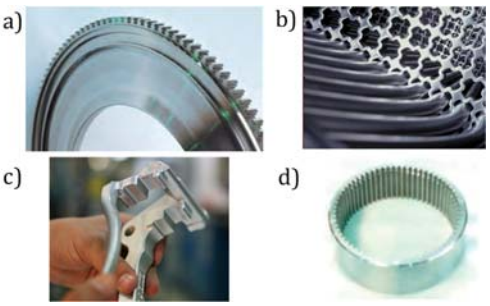


***Figure 4.*** *Examples of broached components: a) fir tree turbine disc, b) quatrefoil shaped hole of tube sheets, c) brake caliper brackets and d) ring gear of an epicyclic gear train.*

## 2. Process fundamentals

The basic principle of broaching is similar to an orthogonal cutting operation and is summarized in Figure 3a. A tool (broach) is composed of several teeth, each of different height $h_b$.

The difference between two heights generates a rise per tooth $h$; that may vary from 80 µm for roughing teeth down to few micrometers for finishing teeth or even zero for calibration teeth (reserve teeth). Chips are generated on the rake face with a rake angle $\gamma$ and stored in a chip chamber (also called "gullet" or "room"). The distance between two teeth is called the pitch $P$. To prevent excessive friction, teeth are sharpened with two clearance angles: $\alpha$ on the relief face and $\alpha_{oe}$ on the flank face. A further description of broaching tool geometries and design is detailed in Section 3.

### *2.1 Research methodology and case studies*

Broaching has been studied in the literature using three complementary approaches. Some authors [4, 11, 37, 80] have used internal broaching machines (Figure 5). Although this process is the most widely used in industrial settings, it is considerably limited from a scientific point of view, as it does not allow the measurement of radial forces.

The second approach argues that radial forces provide valuable information on specific mechanisms governing broaching [26, 67]. In addition, during internal broaching, it is difficult to visualize or monitor chip formation mechanisms, which makes it difficult to optimize. For these reasons, several authors have chosen to study external broaching machines with multiple teeth broaches (Figure 6), which enables the measurement of radial forces and allows clear access to the process for additional instrumentations, using devices such as high speed cameras, infrared cameras and pyrometers [4, 5, 42, 47, 67, 79, 104].

The main limitation of this approach is the rise per tooth, which is predetermined during the broach design. Therefore, multiple broaches are necessary to investigate the effect of rise per tooth.

The final group of authors have employed more fundamental and flexible approaches by using a single tooth (Figure 7) [27, 49, 100, 105].

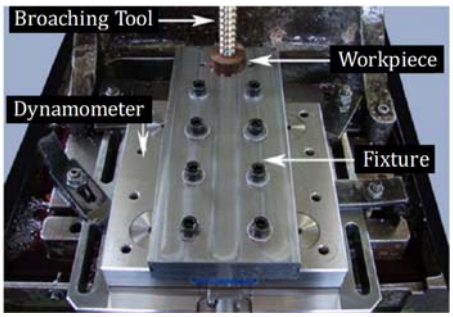


***Figure 5.*** *Internal broaching test* [37].

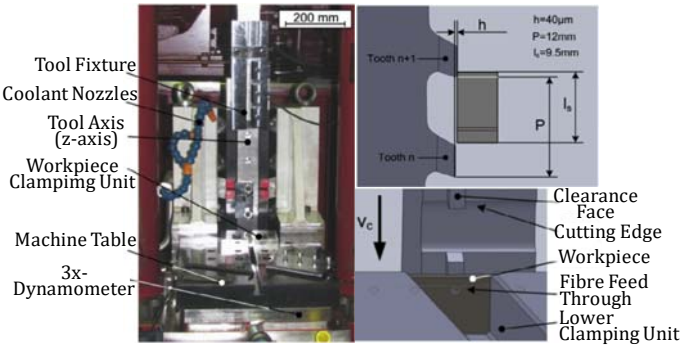


***Figure 6.*** *External broaching test* [42].

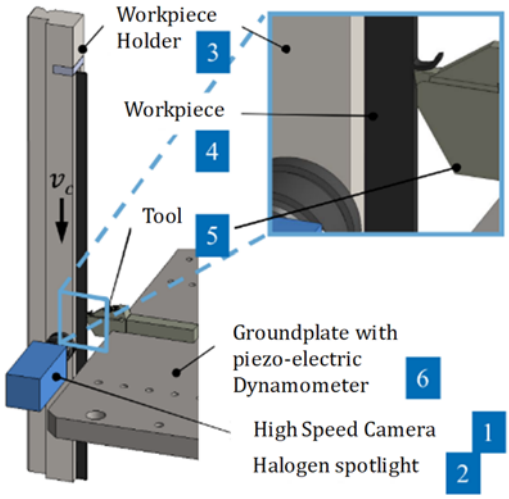


***Figure 7.*** *Broaching investigations with a single tooth* [100].

The aforementioned experimental setups have been widely used when studying steel broaching for automotive components (AISI5115 [11], AISI5120 [78], AISI1045 [29, 37, 104], AISI5115 [56], AISI5120 [66]), or stainless steels for the energy sector (AISI410 [27]). More recently, technological developments have been made with titanium and nickel alloys used in compressor/turbine engines, as a result of the strong growth of the aircraft industry [49, 55, 67].

### *2.2 Chip formation*

Chip formation is one of the key issues in broaching, as the chips which are generated need to be stored in a gullet. Contrary to many cutting processes such as turning, it is not desirable to break chips during a broaching operation. Thus, high rake angles are required to maintain continuous chips. The geometry of the chips is strongly influenced by the cutting speed and the rise per toothv (Figure 8). These parameters tend to increase the curvature of the chip, which leads to wider chips due to a reduction of heat generation at the tool/workpiece interface [27, 29, 49, 78, 79]. To overcome this, the cutting speed is increased, and the corresponding decrease in friction [75] limits the temperature in the secondary shear zone on the rake face, which in turn restricts the thermal expansion of the work material in this zone. An additional benefit is that this reduces chip curvature, allowing the chip to "nest" easily in the gullet.

With regards to the rise per tooth, an increase in this parameter tends to make the chips stiffer, which apart from increasing chip curvature, makes them more difficult to bend. As for the influence of the rake angle, this has a tendency to limit plastic deformation in the primary shear zone and, as a consequence, increase chip curvature.

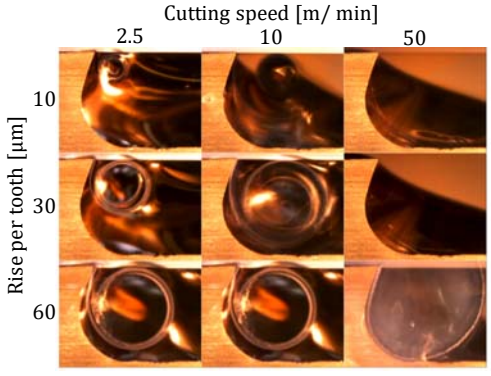


***Figure 8.*** *Chip formation in broaching of X12Cr13 steel* [26].

An increase in cutting speed or rise per tooth increases the productivity. However, both parameters tend to increase the dimension of the chip, which may become an issue as far as chip removal and tooth breakage are concerned (Figure 9). Increasing the productivity thus requires additional mechanical actions to remove chips from gullets (e.g., brushing, high pressure cleaning, etc.) so as to prevent jamming of the chips [4].

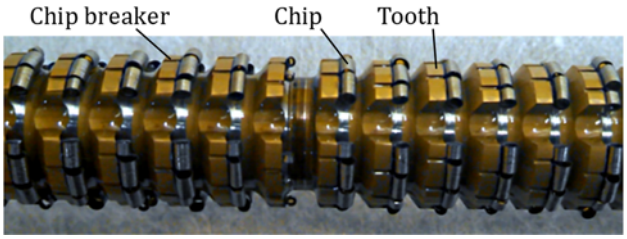


***Figure 9.*** *Chip evacuation problems in internal broaching* [26].

*2.3 Forces*

Broaching operations induce very high forces requiring machines with a rigid structure. These forces are due to the chip load and the high specific forces needed to remove the material. The predetermination of forces in broaching has therefore been systematically studied in a number of experimental investigations. Vogtel et al. [99] focused its attention on the variation of forces during a real broaching operation (Figure 10), of a complex complex-shaped slot. However, such studies are challenging to analyse as each tooth has a different shape of work material to remove. The modelling of the evolution of forces during complex broaching is discussed in Section 7.

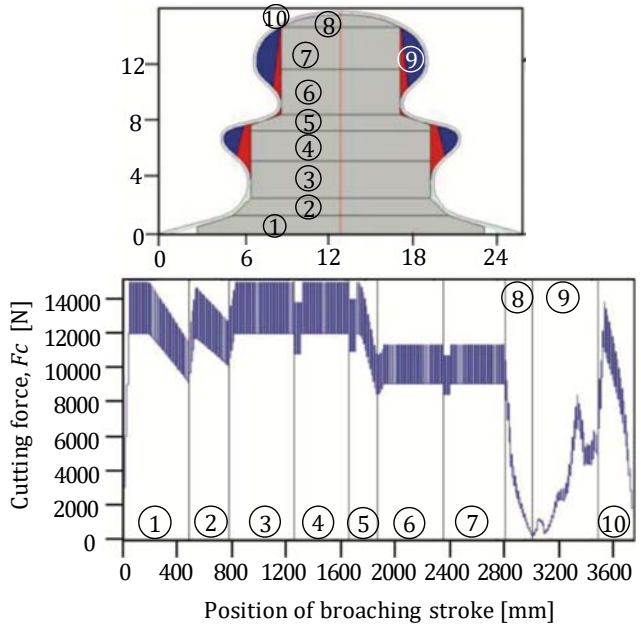


***Figure 10.*** *Change over time of cutting forces during a broaching operation* [99].

Several studies have focused on the variation of forces during a single tooth broaching operation [27, 78, 105]. These studies have highlighted that forces are not constant due to two phenomena: (i) the mechanical system (tool-part-fixturing-machine tool) requires a certain duration to stabilise after the excitation induced by the entrance of the tooth (Figure 11) and (ii) during chip formation, chips damage the gullet and the preceding tooth. Most research has solely analysed stabilized forces (Figure 11) without considering these dynamic attributes of the process.

The macroscopic cutting force *Fc* and radial force *Fr* (also called "penetration" force, "feed" force or "back" force,) are calculated by the addition of both of these aforementioned forces obtained for each tooth in contact with the workpiece simultaneously (Figure 12a).

Many authors have proposed modelling the cutting and radial forces of each tooth based on specific pressure $k_{cc}$ (1) and $k_{cr}$ (2) that are dependent on the work material, tool material, and other working conditions:

$$k_{cc} = \frac{F_c}{A_c} \quad (1) \qquad k_{cr} = \frac{F_{cr}}{A_c} \quad (2)$$

Table 1 sets out the typical order of magnitude of specific pressure $k_{cc}$ for differenet work materials, cutting speeds ($V_c$) and rise per tooth ($h$).

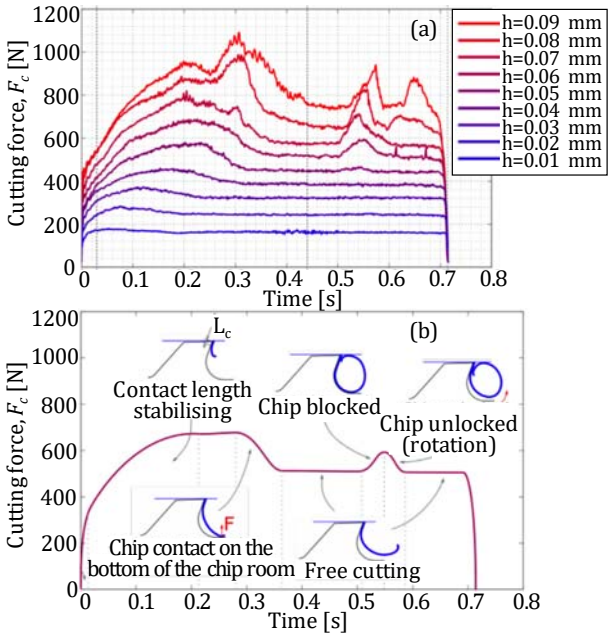


***Figure 11.*** *Influence of a) chip formation and b) chip flow on measured cutting forces* [27].

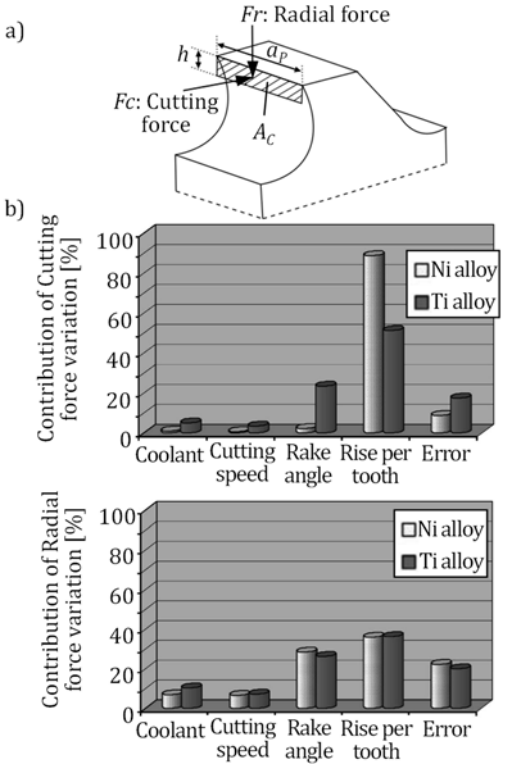


***Figure 12.*** *(a) Forces aplied in a single tooth (b) Influences of various factors to the cutting forces for a single tooth. Data compiled from* [26, 67].

| Material | $V_c$=2.5 m·min$^{-1}$ | | $V_c$=7.5 m·min$^{-1}$ | |
|---|---|---|---|---|
| | $h$=0.015 mm | $h$=0.1 mm | $h$=0.015 mm | $h$=0.1 mm |
| C45 Steel | 3,200 | 2,300 | 3,100 | 2,200 |
| 42CrMo4 | 3,600 | 2,700 | 3,500 | 2,500 |
| 100Cr6 | 5,200 | 3,200 | 5,000 | 3,200 |
| Ti64 | 4,600 | 1,900 | 4,100 | 1,800 |
| Inconel 718 | 7,900 | 4,000 | 10,000 | 3,500 |

***Table 1.*** *Specific pressures $k_{cc}$ (N/mm²) (uncertainty ±10%).*

Fabre et al. [27] and Mo et al. [67] studied the sensitivity of cutting and radial forces (Figure 12b). They identified that cutting force is mainly determined by rise per tooth, whereas radial force (especially $k_{cr}$) is much more sensitive to cutting speed, rake angle and coolant.

There is a growing body of literature which suggests a prevailing trend: forces decrease with cutting speed, rake angle and by adding lubrication (mineral oils) [29, 42, 56, 64, 79]. This trend can be contradicted sometimes, when chip formation interacts with the tooling gullet volume, as reported by [27].

In addition, [13] and [15] observed that a proper choice of broach substrates and coatings may also significantly decrease forces with regard to friction/adhesion between both materials.

### *2.4 Temperature*

Klocke et al. [43] showed that temperatures on the clearance surface of a broaching tool (REXT15 material, cutting edge roundness of 8 µm) could reach values of between 300-500°C, depending on the cutting speed $V_c$ (2.5-10 m·min$^{-1}$), the rise per tooth $h$ (50-150 µm), and the rake angle values $\gamma$ (5-15°), during the machining of forged Inconel 718 (Figure 13). The temperature was measured using a two-color pyrometer with a 320 µm diameter optical fiber. To estimate the temperature on the clearance surface of the cutting tool, the authors proposed the empirical model in Eq. (3):

$$T_{calc,1} = \sqrt[3]{h} \cdot V_c^{0.4} \cdot \gamma^{-0.15} \cdot \sqrt{k_c} \qquad (3)$$

Klocke et al. [41] suggested a modified Komanduri model and Hou model [52–54] for the calculation of the temperature on the cutting edge in the semi-infinite case of broaching nickel-based alloys. Experimental validation of temperature measurements with an infrared camera showed very good correlation (Figure 14).

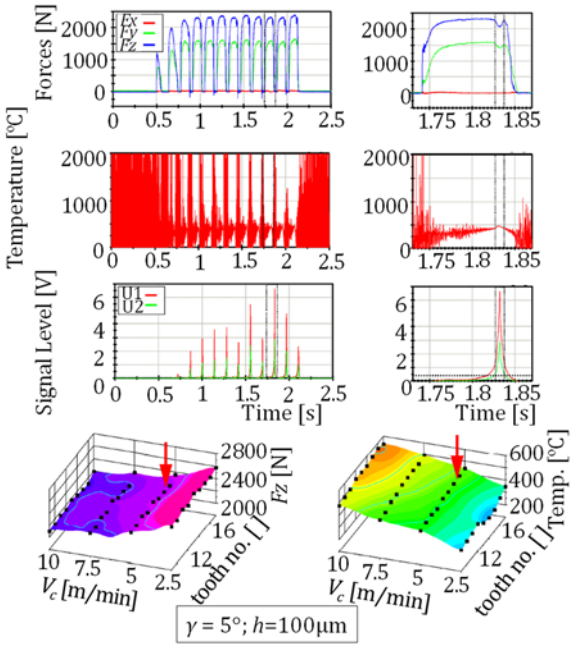


***Figure 13.*** *Temperature in broaching forged Inconel 718* [43].

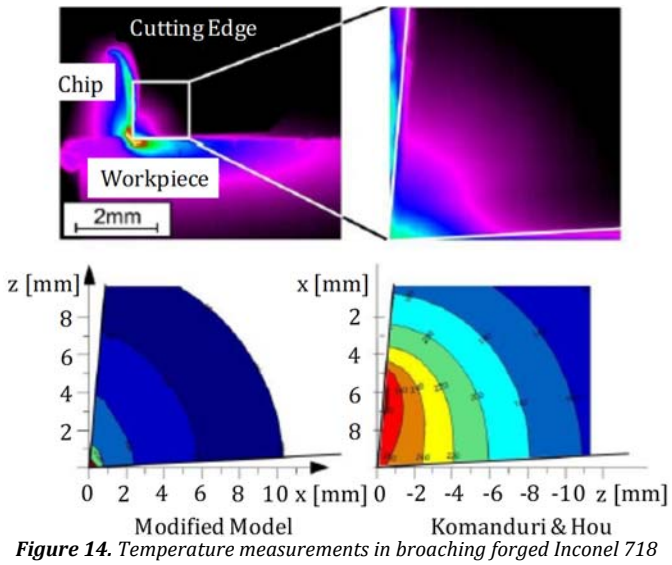


***Figure 14.*** *Temperature measurements in broaching forged Inconel 718* [41].

### *2.5 Roughness*

Surface roughness is one of the key criteria to evaluate a broaching operation. According to Forst [29], the roughness parameter *Ra* may be obtained in the range 1-2 µm. Surface roughness is strongly influenced by several parameters such as: broaching strategy, broach design, cutting conditions, lubrication conditions and work materials [2, 27, 29, 67, 78, 79, 104, 105].

Surface roughness is generated by the finishing teeth (Figure 15a). Depending on the broaching strategy (depth or lateral stepping – Figure 15b), the theoretical surface roughness profiles vary. When the machined surface is parallel to the rise per tooth, a typical triangular profile is generated as a result of the combination of the rise per tooth $h$ and the lateral clearance angle $\alpha$.

When a problem occurs on a single tooth (e.g., grinding defect, wear, unusual adhesion), scratches appear on the surface of the piece (Figure 15c). When the machined surface is perpendicular to the cutting edge, the surface roughness replicates the profile of the cutting edge. Theoretically the profile of the cutting edge is perfect as it is the consequence of the sharpening conditions of the rake face and flank face. However, typical grinding defects observable in Figure 15d may be reproduced on the broached surface. The influence of the broaching strategy on surface roughness has not yet been reported in the literature.

The majority of researchers have studied surface roughness with a basic experimental setup similar to Figure 3a. In this setup the machined surface is generated by the last finishing tooth that prints its profile on the surface. To avoid the consequence of the scattering induced by the sharpening operation, surface roughness is measured parallel to the broaching direction (cutting direction).

By analysing the scientific literature, it is possible to make the following statements:

(i) Surface roughness is highly dependent on the friction properties between the tool substrate and the work material [2]. For instance, among ferritic-pearlitic steels, alloys with a low rate of ferrite lead to a lower friction coefficient, and thus improved surface roughness.

(ii) The presence of free sulphur or graphite in the composition of the work material decreases friction and surface roughness [29, 30].

(iii) Improved surface roughness can be obtained when broaching a single phase material, instead of a multiphase one [27]. The variation of mechanical properties and adhesive properties leads to the apparition of built-up edges, as shown in (Figure 16)

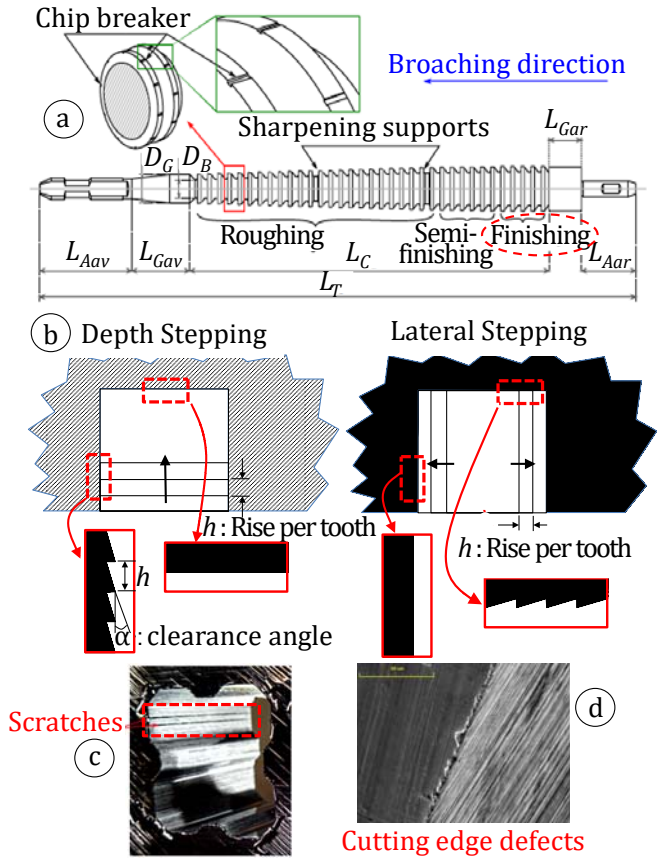


***Figure 15.*** *Surface roughness profile depending on broaching strategy* [26]*: (a) broach design, (b) depth or lateral stepping, (c) example of scratch defects and (d) example of cutting edge chipping.*

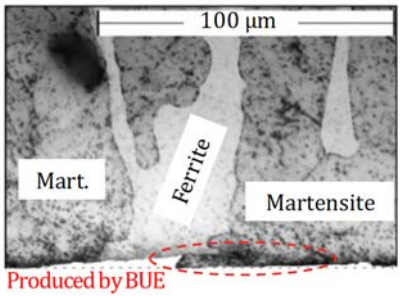


***Figure 16.*** *Influence of ferrite and martensite on surface roughness after broaching an X12Cr13 stainless steel* [27].

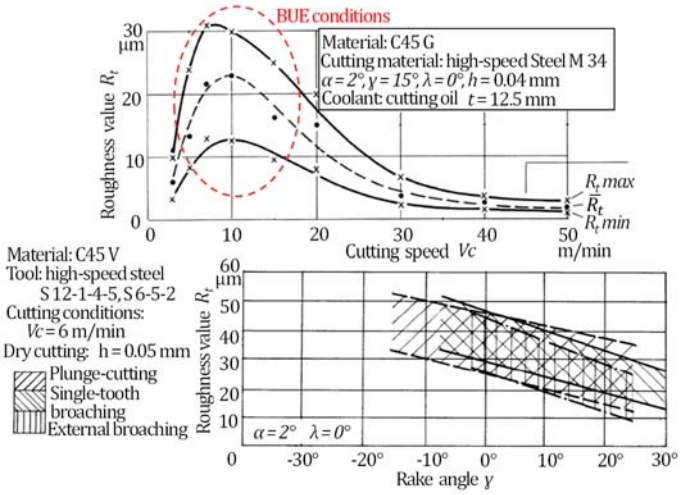


***Figure 17.*** *Influence of cutting speed and rake angle on surface roughness* [29].

(iv) Another way to reduce friction is to increase the cutting speed so as to avoid built-up-edge formation, as shown by [2, 27, 29, 64, 75] (Figure 17).

(v) Lubrication is also a key parameter. Mineral oils provide better surface roughness than emulsion (Figure 18). In contrast, dry broaching leads to poor surface roughness. These results have a high correlation with the highest lubrication property of mineral oil at low sliding speeds as shown by [68]. Among mineral oils, the presence of sulphide and chloride limits adhesion [19, 27], although they are less compliant with recent environmental regulations.

(vi) Broach design also plays an important role in surface roughness. The use of a low rise per tooth for the finishing teeth [27], as well as a high rake angle [29]will help improve the surface roughness (Figure 17).

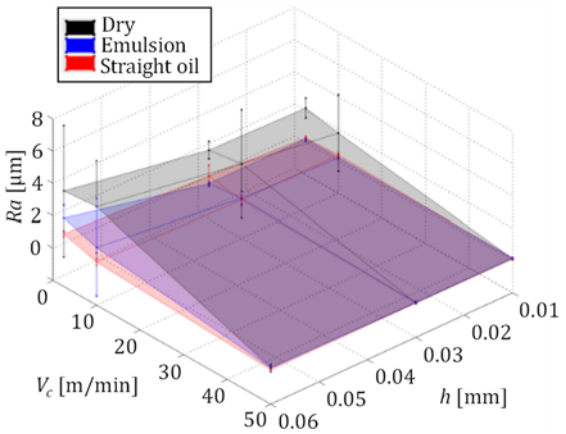


***Figure 18.*** *Influence of rise per tooth, cutting speed and lubrication on surface roughness (X12Cr13 steel)* [27].

Nevertheless, the modification of tool substrate (HSS or carbide) or coating, for a given cutting speed, does not seem to be a key contributor to surface roughness. Hard substrates are mainly required to reach the high cutting speeds that are necessary to decrease adhesion.

### *2.6 Material damage*

The influence of surface integrity on fatigue resistance is a key issue, particularly for safety-critical components. Studies by Chamanfar et al. [18] and Klocke et al. [42] on machined surfaces showed that a layer of around 10 µm is present, affected by thermo-mechanical loads. This layer is composed of ultrafine randomly orientated grains in the first few microns, followed by elongated grains. The thickness of this affected layer can increase depending on the cutting speed. The modification of the microstructure can also be accompanied by an increase in microhardness within a much thicker layer (≈100 µm) (Figure 19).

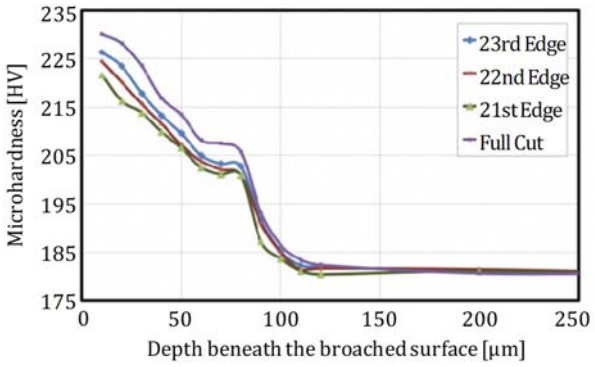


***Figure 19.*** *Change over depth of microhardness for broached AISI12L14* [37].

Chen et al. [20] analysed the characteristics of the white layer obtained in a forged disc of Inconel 718, which was solution heat treated and air cooled. The broached white layer consisted of a nanocrystalline structure with a strong sheared texture, and a grain size in the range of 20–50 nm. The microstructural and crystallographic features of the broached white layer suggest that it was essentially formed by adiabatic shear localization, in which the dominant metallurgical process was rotational dynamic recrystallization based on mechanically-driven subgrain rotations. The grain refinement within the white layer increased the surface nano-hardness by 14%. However, it also caused a reduction of almost 10% in the elastic modulus compared to that of the bulk material.

### *2.7 Residual Stress*

Authors who have focused their attention on residual stress, [18, 66, 81, 105] have observed that generally tensile residual stress is present in the external affected layer (Figure 20). This indicates that thermal mechanisms are dominant in broaching [76]. Nevertheless, in comparison with polished samples, Chen et al. [21] observed that a beneficial effect of the broaching operation was found on the fatigue life (Figure 21) which could be related to the high compressive residual stresses obtained below the broached surfaces (Figure 22).

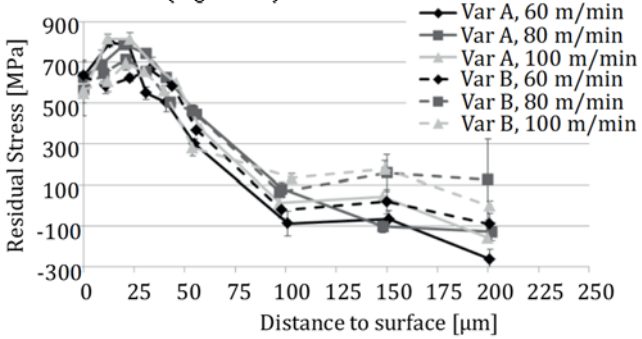


***Figure 20.*** *Change over distance to surface of residual stresses in AISI5120* [66].

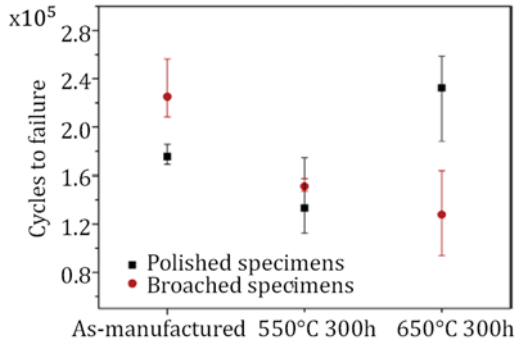


***Figure 21.*** *Fatigue lifetime obtained from bending fatigue tests* [21].

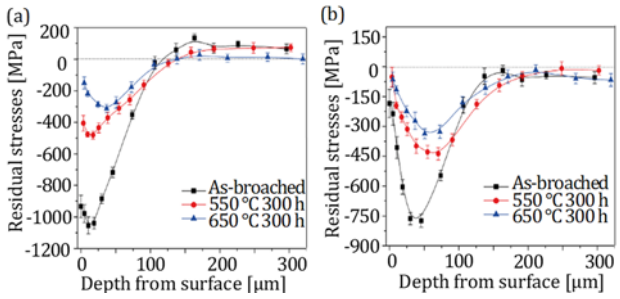


***Figure 22.*** *Compressive residual stresses induced by broaching and stress relaxation after heat treatments: (a) longitudinal direction; (b) broaching direction* [21].

### *2.8 Burrs*

Burrs are likely to occur when broaching ductile materials (e.g., steels, stainless steels, titanium alloys, nickel alloys). Surprisingly few studies have investigated the minimization of burrs, and thus in practice a deburring operation is typically necessary.

### *2.9 Dynamics*

The dynamic behaviour of the system "Machine+Broach+Part" may affect the quality of parts, as shown by [5, 67, 100, 105]. The entrance and exit of teeth induces a sudden variation of forces that in turn gives rise to an oscillation of the system. This causes visible variation of the surface roughness (Figure 23). These phenomena may become even more problematic when the cutting speed is increased, which is contrary to the expectation of improved surface roughness as outlined in Section 2.5. To limit the consequences of these step by step increases in the cutting forces, some authors recommend using broaches with variable pitch between the teeth [13].

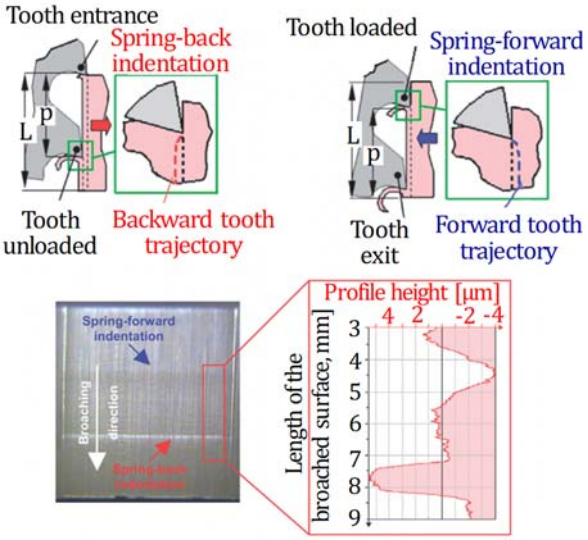


***Figure 23.*** *Influence of tooth entrance and exit on surface roughness* [5].

### *2.10 Dimensional tolerances*

Broaching has the potential to produce highly accurate geometries up to IT7. The geometrical accuracy of broaching is dependent on the radial forces, the corresponding deflection of walls and the local deformation of teeth. Therefore, an accurately finished surface requires a low radial force [11, 26, 67], which is mainly possible when low rise per tooth and high cutting speeds are employed (Section 2.3).

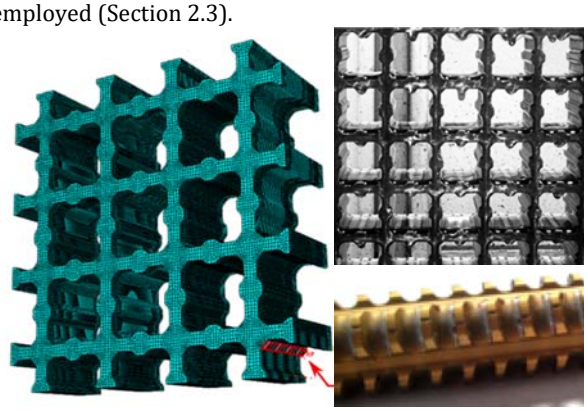

***Figure 24.*** *Numerical modeling of deformation of a part due to broaching forces* [26].

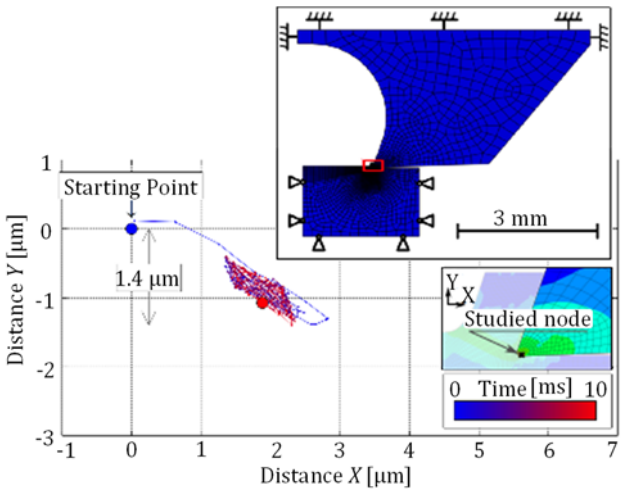


***Figure 25.*** *Numerical modeling of teeth deformation due to forces* [26].

As for part design, accuracy (i.e., deflection) is strongly related to the stiffness of the part, which depends on the geometry (i.e. wall thickness) and the elastic modulus of the work material. The complexity of the problem implies that such errors can best be quantified with finite element calculation (Figure 24) [11, 26, 97]. With regards to the local deformation of teeth, the magnitude is typically limited to 1 or 2 µm for finishing teeth when the depth of cut (rise per tooth) is lower than 10 µm [26, 97] (Figure 25).

### *2.11 Wear*

Wear is generated in broaching by the friction between the clearance face of the tooth and the machined surface, and by the friction between the rake face and the curling chip. Wear mechanisms in broaching are particular as cutting speeds and chip thickness values are much smaller than in other common cutting processes (e.g., turning and milling). Moreover, broaches have an exemplary design with high rake angle, a sharp edge, and they usually lack coating on the rake face (as a result of resharpening). Adhesive wear and abrasive wear are the main mechanisms observed. The presence of adhesion does not facilitate the diagnosis and quantification of wear. Furthermore, few scientific investigations have been undertaken, as wear testing in a laboratory is time-consuming and costly. Some studies, such as [67], have reported results without being able to generalise any specific trend. Burnett, et al. [17], have identified a correlation between hardness and wear for ferrrite/pearlite steels. Klocke et al. [49] presented a sensitivity study of broaching an Inconel 718 alloy with carbide broaches, and showed that chipping is a major wear phenomenon when high clearance angles or low rise per tooth are used due to the brittleness of the carbide substrate.

Studying broaching under real factory conditions requires even longer and costlier tests, as real parts need to be machined. In addition, the large number of teeth in an industrial broaching process makes it difficult to take individual measurements and requires a special setup [62]. Such approaches are often limited to tool manufacturers [29] and the results frequently remain confidential. An example of comparison between a High Speed Steel (HSS) and a carbide broach is presented in Figure 26.

As far as end users are concerned, they tend not to monitor wear but rather focus their attention on the quality of the part (i.e., evolution of roughness, part accuracy), or on production disturbances (i.e., chip adhesion in gullets between two cuts, vibrations, overload on cutting forces). The monitoring of these parameters is discussed in Section 6.

### *2.12 Key Parameters: qualitative sensitivity study*

Table 2 summarizes the key parameters for some fundamental and industrial outcomes obtained from the literature. A study of this table would indicate that the key parameters in the broaching process for roughness and cutting forces are the following: rake angle, cutting edge finishing, cutting speed, rise per tooth, and cutting fluid [26, 27,29].

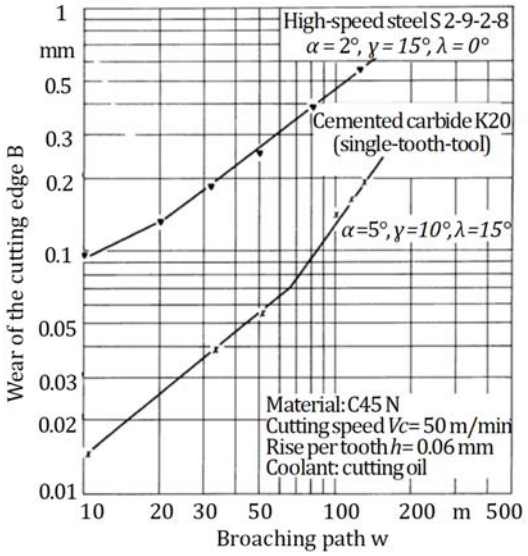


***Figure 26.*** *Evolution of wear in broaching for two substrates* [29].

| | | FUNDAMENTAL VARIABLES | | | | | | | | | | INDUSTRIAL OUTCOMES | | | | | | |
|---|---|---|---|---|---|---|---|---|---|---|---|---|---|---|---|---|---|---|
| | | Cutting Force | Penetration Force | Lateral Force | Workpiece Temperature | Tool Temperature | Chip Temperature | Stresses on the tool | Tool Chip Contact Length | Pressure on the tool | Vibrations | Surface Roughness | Material damage | Residual stress (Positive) | Dimensional Tolerances | Burrs | Tool life | Chip evacuation |
| ++ | Significant Worsening | | | | | | | | | | | | | | | | | |
| + | Worse | | | | | | | | | | | | | | | | | |
| | Not clear | | | | | | | | | | | | | | | | | |
| - | Improvement | | | | | | | | | | | | | | | | | |
| -- | Significant improvement | | | | | | | | | | | | | | | | | |
| 1-Cutting Tool | Rake angle (negative to positive) | - | - | -- | - | - | - | - | + | ++ | - | -- | - | | - | - | + | - |
| | Clearance angle (zero to positive) | - | - | - | - | | | | | | | | | | | | | |
| | Skew angle (zero to positive) | - | - | ++ | | | | | | | | - | | | - | | - | |
| | Cutting edge radius (zero to positive) | + | ++ | + | | + | | - | | - | + | + | + | - | + | + | + | |
| | Uncoated > Coated | - | - | -- | - | - | - | - | - | - | - | - | - | | - | - | -- | - |
| 2- Cutting Condition | Cutting speed (zero to positive) | | | | - | ++ | + | + | + | + | + | * | ++ | + | | - | + | |
| | Rise per tooth (zero to positive) | ++ | ++ | -- | -- | + | + | + | ++ | | + | ++ | ++ | + | - | - | + | + |
| 3- Lubricant | Dry > Water soluble > Oil | - | -- | - | - | - | - | - | - | - | | -- | | | | | -- | |

**Nonlinear behaviour: at low cutting speeds (<10m·min$^{-1}$), an increase of cutting speed worsens the roughness and for high cutting speeds (>10·min$^{-1}$), an increase of cutting speed improves the roughness.*

***Table 2.*** *Key parameters influencing fundamental variables and industrial outcomes* [26, 27,29].

## 3. Broaching tool materials and tool design

### *3.1 High speed steel*

Broaching tools usually work at low cutting speeds and thus High Speed Steel (HSS) tool materials are commonly employed. The selection of HSS type would typically depend on the work material to machine and machining application [95].

For easy to cut materials (e.g., aluminium, magnesium, free-machining steels, with tensile strength, $R_m$<800 MPa), conventional HSS are used and combined molybdenum, tungsten, and chromium as the main alloying elements. The most common is denoted as M2 and has small and evenly distributed carbides giving high wear resistance. After heat treatment, this material reaches a hardness of 63-65 HRC.

For cutting steel, stainless and cast iron ($R_m$<1,000 MPa), cobalt based HSS tool materials such as M35 (5% Co) and M42 (8-10% Co) are the standard choice. The addition of cobalt provides an increased heat resistance and permits a hardness of at least 67 HRC to be achieved. Depending on the cobalt content, cobalt based HSS steels are also denoted as HSS-E or HSS-Co. Higher cutting speeds can be achieved with these tool materials in comparison to conventional HSS.

Powder metallurgy processed HSS-PM (e.g., ASP-2015, ASP-2023, ASP-2030, ASP-2052, ASP-2060) provides a more homogeneous microstructure with a low grain size and higher alloying capability, thus increasing hardness. When these HSS-PM are subjected to hardening treatments in vacuum furnaces, hardnesses of 68-70 HRC can be reached. HSS-PM tool materials can also achieve higher productivity and tool life than conventional HSS, and are thus suitable for machining titanium and nickel-based alloys. Typical attainable cutting speeds are listed in Table 3 for different combinations of HSS broach tool and workpiece materials [95].

An increased performance of HSS and HSS-PM tool material can be achieved by surface modification and application of PVD coating; typically TiN (improved abrasion resistance), and TiALN or AlCrN (high cutting speed, high productivity in steel broaching) [32, 57, 61, 95].

| Workpiece material | HSS broach | HSS-Co broach | Coated HSS-PM broach |
|---|---|---|---|
| Steel | 3-8 | 3-10 | 3-60* |
| Stainless steel-tough | 2-5 | 2.5-4 | 2.5-5 |
| Stainless steel free machining | 4-6 | 4-8 | 4-10 |
| Cast iron | 8-10 | 8-12 | 8-60* |
| Brass | 8-10 | 8-12 | 8-60* |
| Bronze | 8-10 | 8-12 | 8-60* |
| Aluminium | 8-10 | 8-12 | 8-60* |
| Magnesium | 8-10 | 8-12 | 8-60* |

***Table 3.*** *Attainable cutting speeds for a combination of HSS broach and workpiece materials. (*) A special broaching machine is required for high cutting speeds* [95].

### *3.2 Cemented carbide*

In comparison to HSS, cemented carbides have higher hardness and heat resistance, but lower fracture toughness.
Although the latter can make cemented carbides more susceptible to edge chipping than HSS during tool entry, their overall increased abrasive wear resistance is essential to be able to work at high cutting speeds. Generally, a balance between high toughness and wear resistance can be achieved by selecting a high cobalt content grade with a coarse grain structure (e.g., WC-13%Co, 1.7 μm grain size, HV1300) and PVD coating (e.g., TiN-TiALN).

Examples of cemented carbide broaching tool types are shown in Figure 27, illustrating three different concepts: (a) multi-edge insert (MEI), (b) modified triangular insert with 2 cutting edges, and (c) square insert with 4 cutting edges (left/right). These types of carbide broaching solutions are employed in the aerospace and power generation industries for the manufacture of profiled grooves in compressors and turbine discs. Their application is limited to roughing, and medium machining, and semi-finishing with cutting speeds typically $V_c$= 20-25 m·min$^{-1}$ for Ti6Al4V alloy; $V_c$ =10-15 m·min$^{-1}$ for Inconel 718 nickel-based alloy and $V_c$=60 m·min$^{-1}$ for steel. Other distinct advantages of a cemented carbide insert broaching solution over HSS are the utilisation of up to 4 edges per insert and the elimination of the need for regrinding operations.

Klocke et al. [40] reported on the performance of cemented carbide grades during rough broaching and manufacture of profiled grooves in an Allvac 718 Plus nickel-based alloy. Their results indicate that rough broaching with cemented carbide tools using indexable inserts can be performed successfully at cutting speeds up to five times higher than the cutting speeds applied in industrial applications with HSS tools (Figure 28).

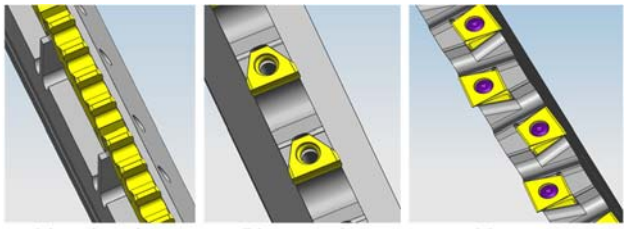


***Figure 27.*** *Examples of cemented carbide indexable insert broaching tool concepts* [84].

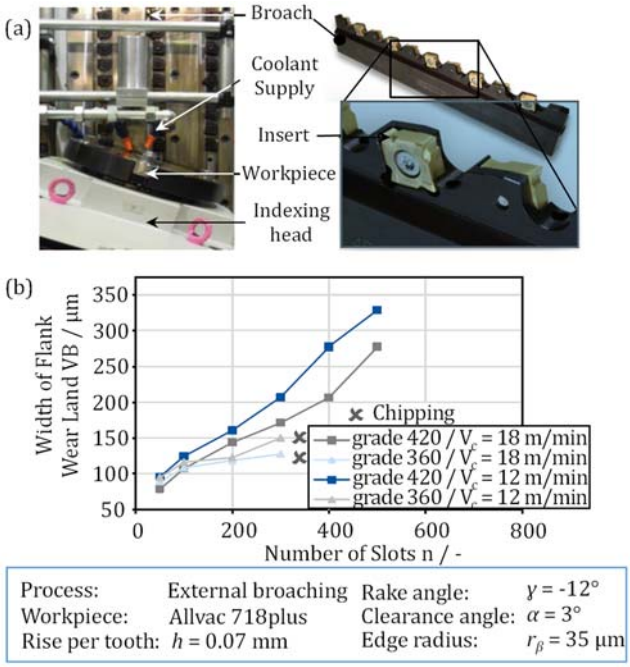


***Figure 28.*** *Performance of cemented carbide broaching tools in broaching Allvac 718 plus. (a) Experimental setup for broaching of Inconel (left) and worn broaching cemented carbide tool (right) and (b) Tool life tests with varying cemented carbide Seco grades 360 (WC-15%Co, 0.9 μm grain size, HV1375) and 420 (WC-13%Co 1.7μm grain size, HV1300)* [40].

### *3.3 Geometry and design of broaching tools*

Broaching tools are individually designed to match the desired profile to be produced in the workpiece material. Figure 3c shows some examples of broached profiles and their corresponding tool geometry in internal broaching [36]. The complexity of the broaching tool design can vary from designing a simple broach for a keyway to a more complex tool profile to manufacture a fir tree

curve shaped profile in a turbine disc. The types of broaching tools can be classified into the following groups [28]:

- Round broaching tools: employed in internal broaching. These can be involute spline, helical spline, serration, parallel straight sided, cam-form, or irregularly shaped internal splines with either annular or spiral tooth forms.
- Flat or rectangular shaped broaches: employed in external broaching.
- Keyway broaches: used for cutting single or double drive keys in gears or pulleys.
- Blind spline broaching tools: used in applications that do not allow a conventional internal or external broach to pass over or through a part.

Figure 3a displays a typical side profile for a HSS broaching tool with its associated geometrical features, i.e., pitch length ($P$), tooth height ($h_b$), land ($L_D$), rake angle ($\gamma$), clearance angle ($\alpha$), and rise per tooth ($h$). The definition and characteristics of these tool geometrical attributes are set out below [34]:

- *Tool Length*. The length of a broaching tool is determined by the amount of material to be removed and the mechanical properties of the workpiece.

- *Pitch Length*. Pitch length ($P$), is the distance between two successive teeth on a broaching tool, which is determined by the cutting length and greatly influenced by the type of workpiece material. It is advisable that at least 2-3 teeth are simultaneously engaged in the workpiece. To prevent pitch marks on the finished surface, two or three different pitches of unequal length are used.

- *Land Length*. The thickness of the tooth at its tip level is called land length ($L_D$), and determines the ability of the tooth to withstand cutting stresses.

- *Rake Angle*. Rake angle ($\gamma$), is the angle between the cutting face and the normal direction of the workpiece surface. The rake angle in broaching tools is normally positive, reducing the power requirement and enhancing chip flow over the rake face. However, for certain cast iron and hard broaching applications, it can also be negative. To achieve a balance between having moderate cutting forces and sufficient strength to ensure proper tool life, the rake angle must be selected within the optimum range (see Table 4).

- *Clearance Angle (Relief Angle).* The clearance angle ($\alpha$), is the angle between the back of the tool and the horizontal line (normally parallel to the machined surface). The clearance angle is designed to provide sufficient space between the workpiece and back of the tool to eliminate interference and reduce friction. The clearance angles for different broaching tools are reported in Table 5. It is important to note that resharpening is achieved by grinding the rake surface, and this means that the finishing cutting edges could lose dimension in the lifetime of a tool, comprising successive resharpening. As shown in Figure 29, for each $a$ mm that is sharpened, $b$ mm is lost.

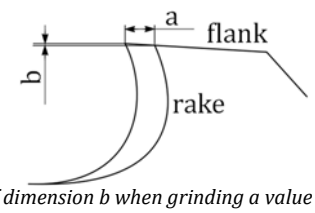


***Figure 29.*** *Loss of dimension b when grinding a value in the rake surface.*

- *Rise Per Tooth*. The rise per tooth ($h$), also known as tooth rise or feed per tooth, is the difference between the heights of the two successive teeth which determines the undeformed chip thickness or depth of material to be removed by each tooth.

- *Gullet Space*. The empty space between two successive teeth defined by ($r_1$) and ($r_2$) is known as Gullet Space (Figure 3a). Gullet space is mainly used to retain the chip during cutting until the tooth leaves the workpiece. To prevent chips from jamming, the gullet space must be 6 times larger than the chip volume. Tool breakage may occur when the gullet space is too small, and in such cases poor surface finish can be caused by the removed chip rubbing on the machined surface. In contrast, a large gullet space makes the tooth very slender and decreases the strength and stability of the broaching tool.

| | Rake angle $\gamma$ (°) | |
|---|---|---|
| Work material | Roughing | Finishing |
| Steel | 15 | 5 |
| Grey cast iron | 10 | 5 |
| Malleable iron | 10 | -5 |
| Aluminium and its alloy | 20 | 20 |
| Bronze and brass | 5 | -10 |

***Table 4.*** *Rake angle for roughing and finishing teeth of broaching* [34] .

| | Clearance angle $\alpha$ (°) | | |
|---|---|---|---|
| Type of broach | Roughing | Semifinishing | Finishing |
| Round and spline | 3 | 2 | 1 |
| Keyway | 3 | 2 | 2 |
| External | 3 | 2 | 2 |
| Adjustable table | 3-4 | 3-4 | 3-4 |
| Nonadjustable table | 3-4 | 2 | 1-2 |

***Table 5.*** *Clearance angle for roughing, semifinishing, and finishing teeth of broaching tools* [34].

- *Helical broach/skew angle:* The use of helical broaching (internal) or skew angles (Figure 30) provides improved force balancing during the broaching process, which in turn facilitates high accuracy and longer tool life.

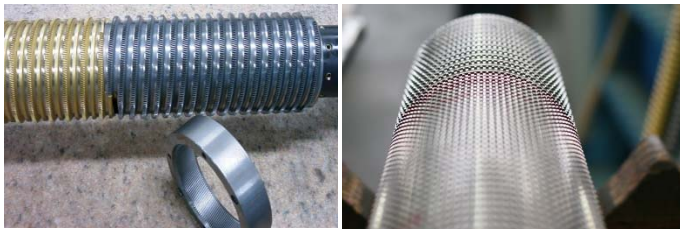

***Figure 30.*** *Helical and straight broaching tools.*

- *Cutting edge finishing.* Although the finishing of the cutting edge seems to be one of the most relevant in broaching, especially considering the low values of the rise per tooth in the finishing teeth, no publications were found analyzing this parameter. Its increase is linked to an increase in all the forces, and particularly penetration forces. Its value can be in the range of 1 to 10 microns, with the lowest values corresponding to the finishing teeth.

- *Chipbreakers.* Chipbreakers are used to prevent chip packing and facilitate chip removal by breaking them. In internal broaching processes, the broach produces ring-shaped chips that would wedge in the tooth gullet, and eventually cause the tool to break if chipbreakers were not employed. Chipbreakers ground parallel to the tool axis and manufactured on alternate teeth are staggered so that each set of chipbreakers is followed by a cutting edge. This solution helps ensure that the material not removed by one chipbreaker is removed by the following one. Another reason to use a chipbreaker is because chips tend to swell in width when cut, and if left unbroken could roll inside the gullet space, worsening the surface roughness. If the tooth has a chipbreaker, the chip will be split into two and will move inwards (Figure 31), preventing rubbing on the flank of the profile.

As a large number of geometric features need to be considered in the design of a broaching tool, several studies have focused on developing computer aided design and cutting force modelling approaches to optimise broach tool design for particular workpiece profiles [1, 34, 72, 74, 94, 99].

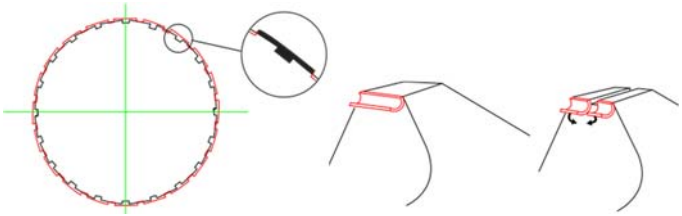

***Figure 31.*** *Chipbreakers in a broaching tool.*

An example of this can be found in the work of Vogtel et al. [99] who developed broaching tool design software with a graphical user interface (Figure 32) to cut a user-defined complex-shaped slot. This method generates a cutting strategy for the broach with a set of technological constraints, such as maximum allowed cutting force per tooth or maximum allowed rise per tooth. Using this methodology, it is possible to obtain the optimal length of the tool, thus reducing tool manufacturing costs and machining time [99].

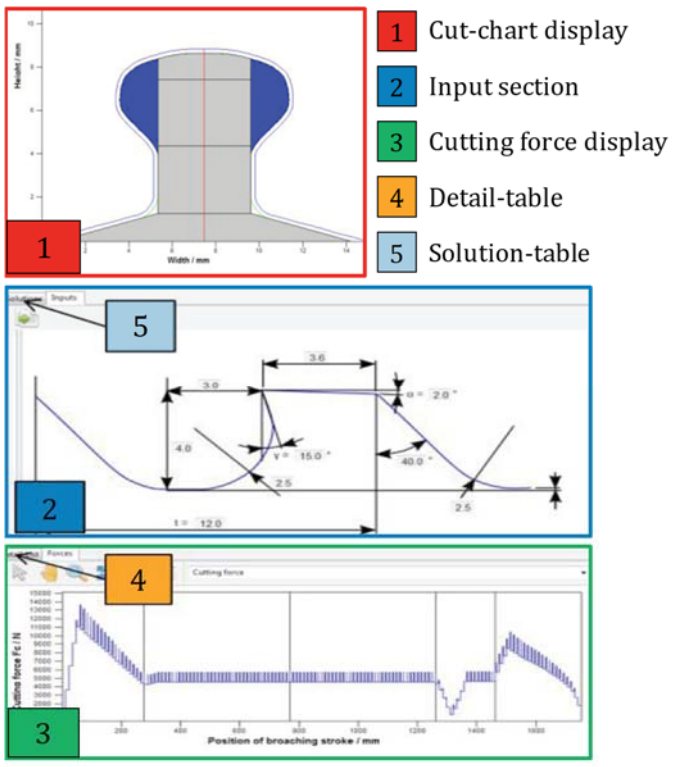


***Figure 32.*** *Overview of the graphical user interface for automatic broaching tool design* [99].

### *3.4 Manufacturing / Resharpening*

The manufacture of broaching tools is a complex process as in some cases lengths of 3.5 m and diameters of 400 mm are required. The manufacturing process of HSS broaching tools is primarily based on the following operations:

- Roughing in green conditions of the material by milling and turning.
- Heat treatment (up to 68-70 HRC).
- Grinding on 5-6 axis machine tools in thermally controlled workshops. The selection of the grinding wheel and cooling conditions requires careful consideration.
- Coating applications.
- Final grinding to sharpen the tools (Figure 33) and obtain the required dimensions.
- Cutting edge finishing by brushing [22].

***Figure 33.*** *Final grinding of a broaching tool* [90].

## 4. Fixture systems

Although fixturing systems are related more to engineering aspects rather than machining science, they play a crucial role in achieving the desired quality of the finished part (i.e., dimensional/geometrical accuracy). Even if significant resources are allocated for the machine tool and broaching tools, if the fixturing system is not appropriately designed, the process outcomes can be significantly off-target. Nevertheless, there is very limited in-depth information available as to how to map the specific requirements of the broaching process against the design rules for fixturing systems. As the broaching tool and the workpiece have a linear relative movement, it is critical that these are aligned with a high degree of accuracy. Failure to do so can not only lead to deviations from the required quality of the finished part, but also to tool damage (e.g., tooth breakage). In this context, the term fixturing systems refers to solutions related to both broaching tools mounted on the machine ram, as well as the part mounted on the machine table.

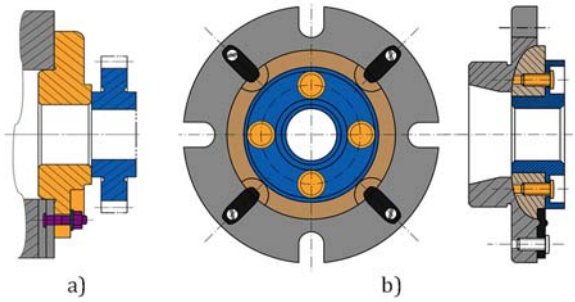


***Figure 34.*** *Examples of part holding systems for broaching: (a) simple location which requires a high degree of tool-workpiece accuracy ; (b) concept for self-alignment* [25, 89].

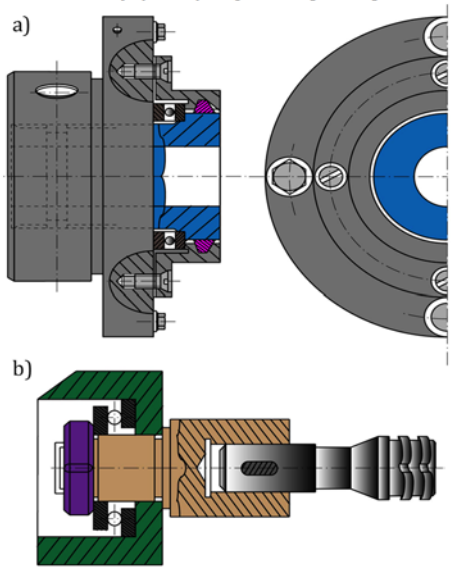


***Figure 35.*** *Examples of holding systems with part (a) and (b) tool rotation to broach helical internal channels* [25, 89].

Considering that long broaching strokes require a high degree of tool-workpiece alignment, there is a need to allow the parts to self-align against each other, for which special part fixtures exist (e.g., spherical surfaces) (Figure 34a). If such solutions are not adopted, and a conventional part fixture is used (Figure 34b), then mounting the tool and the part on the broaching machine will require an exceptional degree of accuracy.

In addition, part fixtures can be designed to allow even more complex profiles than those resulting from the linear movement of the tool. As an example, the part holding system can allow rotation that in combination with an appropriate broaching tool geometry, could enable the generation of internal helical channels (Figure 35). Thus, the fixture system adds to the kinematics of the process, which in turn enhances the capacity of the process to generate more complex surfaces. Fixtures for broaching tools, usually employing guides and bolted clamps (Figure 36a), need to ensure a tight tolerance in alignment with the machine ram, whilst being able to withstand considerable reaction forces from the broaching process. Nevertheless, when the broaching teeth present a skew angle, the fixtures need to allow the lateral reaction forces to be orientated towards high stiffness locators (i.e. mechanical elements, such as pins, that replicate supporting points which are associated with the restriction of degree of freedoms to enable the orientation of the part in the 3D space, Figure 36c). In certain broaching profiles (e.g., internal splines) resharpened tools cannot be used. However, in some other applications, such as key slots, the use of resharpened tools is possible, as long as the adjustments of the relative position between the tool and the workpiece are considered. Figure 36b depicts a solution for height compensation of the tool after resharpening.

In practice, the design of fixtures for both tool and part need to match their relative position to a high degree of accuracy (see Figure 37).

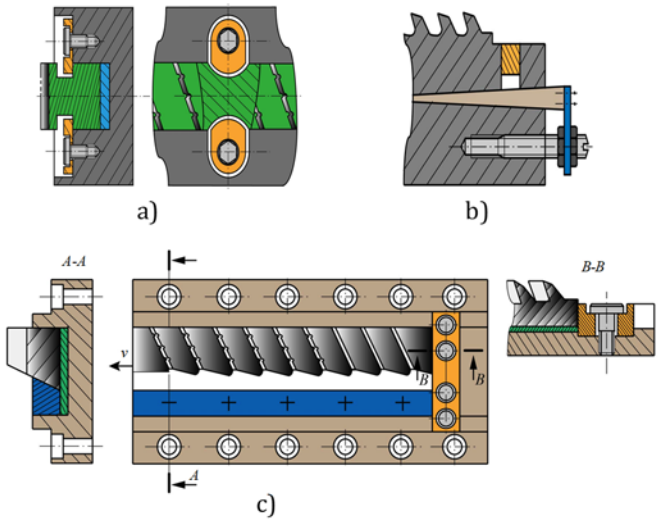


***Figure 36.*** *Examples of holding systems for broaching tools:a) symmetrical clamps, b) system allowing the height adjustment to compensate for broach resharpening and c) system for broach with inclined cutting edges* [25, 89].

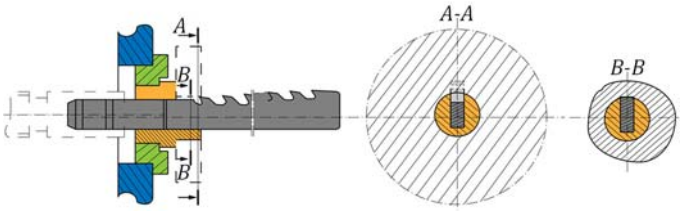


***Figure 37.*** *Examples of holding systems to broach key slots* [89].

## 5. Machine tools

Broaching machine tools can be classified as follows:

- *Orientation: vertical and horizontal*. Vertical broaching machines take up less space than horizontal ones. In general, interior broaches are usually vertical (e.g., Figure 38). The main reason for using horizontal machines is because long strokes are required for complex shapes. It is also quite common to use horizontal broaching in external operations for components, such as steering racks and turbine discs (e.g., Figure 39). Horizontal broaching machines present a significant advantage over their vertical counterparts, in which the influence of inertia due to gravity is minimized on the panel that can weigh more than 3 tons.


***Figure 38.****Vertical broaching machine* [24].


***Figure 39.*** *Horizontal broaching machine*

- *Workpiece / tool movement.* In most machine tools the moving part is the workpiece. Advantages of this configuration are that less space is required compared to external broaching machines (Figure 40), and there is no need for a pit, as is the case for inner broaching tools (Figure 41). This eases restrictions on the design and modification of layouts in a production plant.

- *Actuation system: hydraulic/electro mechanics.* Broaching machines have traditionally utilized hydraulic systems, but in recent years electromechanical broaching machine tools have become increasingly common. This is because the use of programming enhances position control and cutting speed profiles, and energy consumption and noise can be reduced by up to 50%. In addition, new data capture systems which monitor the machine components and subsystems (motors, regulators, position sensors, load cells, etc.) together with the ability to provide teleservice, means that modern broaching machines have entered the world of Industry 4.0, with all its associated advantages.

Nevertheless, the use of a hydraulic pump is still considered essential in broaching machines to provide support to the fixture and transfer system of the components. In some broaching machines the hydraulic group is separated from the structure to prevent the structure from overheating.

The essential advantage of hydraulic broaching machines lies in their simple design and ability to accurately deliver the cutting forces necessary in broaching. This technology is still the most commonly used in industry, even though new designs based on electronic control are now commonplace.

Current electromechanical broaching machine tools have similar power to hydraulic ones. The cutting force usually range from 10, 25, 63, 100 and even 120 tonnes. The speeds, in conventional broaching, range from 2 to 30 m·min$^{-1}$. In hard broaching they are around 60-80 m·min$^{-1}$ and in dry about 35 m·min$^{-1}$.

There are different types of actuation mechanisms used in electromechanical broaching machine tools:

- Chain and notched wheel.
- Planetary spindles.
- Ball screws.
- Rack and pinion.
- Rack and chevron pinion.

The rack and pinion option is frequently employed when significant cutting forces (40-120 tonnes) and high cutting speeds are required, while the system employing screw recirculating rollers transmits lower forces (≈10-40 tonnes).

Broaching machine tools carry a high cost – in the range of €1.5M. This is because they must perform many cycles in their worklife, maintaining precise guidance adjustments (ensuring a process capability index of more than 2.33) and withstanding extreme forces and inertias (there exist broaching machines that generate forces of up to 100 tonnes and cutting speeds of up to 100 m·min$^{-1}$).

Figure 42 sets out the classification of broaching machine tools.

***Figure 40.*** *External broaching machine equipped with a robot* [24].

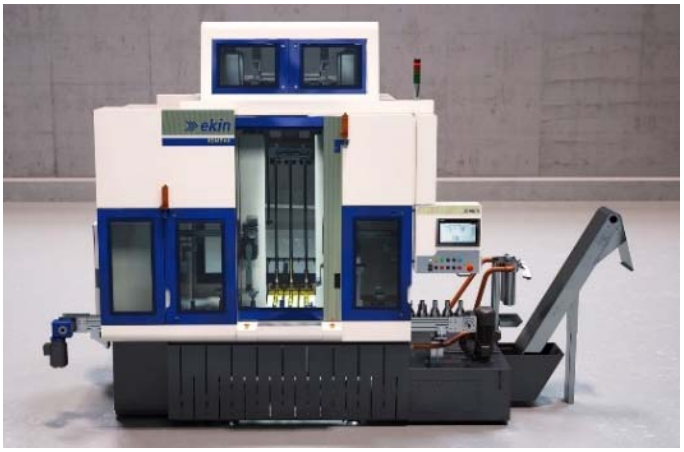

***Figure 41.*** *Internal broaching machine tool* [24].

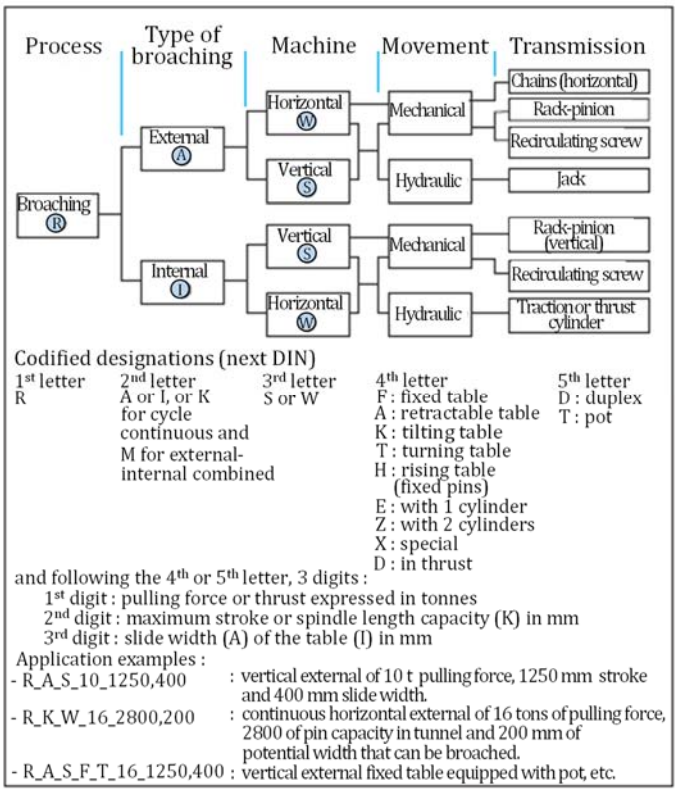


***Figure 42.*** *Classification of broaching machine tools* [12].

## 6. Process monitoring

In contrast with other machining processes in which the cutting process with similar characteristics is repeated in the time domain, process monitoring in broaching is a challenging task. This is due to the uniqueness of the tool design with non-identical tooth geometry. For this reason, sensory signals need to be correlated to the specifics of the cutting mechanisms and tooth geometry at a certain moment in time, to derive dependencies that allow detection of process malfunctions. To make signal analysis even more challenging, at any given time more than two teeth of non-identical geometry could be in contact in the workpiece; and hence, some "cumulative" signals (e.g., forces, vibrations, etc.) need to be carefully interpreted to understand which cutting edge may have generated a certain process malfunction. Thus, monitoring solutions in broaching have focussed on detecting process malfunctions occurring at both tool and workpiece surface levels. Of course, if the former occurs it is most likely to be manifested by the generation of workpiece surface damage as well.

### *6.1 Tool condition monitoring*

Cutting forces can be used to detect tool malfunctions (e.g., wear/chipping of cutting edges) either by utilising off-the-shelf dynamometers [7] or embedding sensors in the machine structure. The latter could be considered more suitable for industrial applications. Cutting force signals can be analysed by averaging their peak values for each cutting edge against cutting time and defining experimentally calibrated relationships with flank wear of the cutting edges [7, 10, 67, 100]. This approach is efficient to monitor wear of cutting edges of similar geometries belonging to a single tooling segment (e.g., broaching spline). However, it is more difficult to implement when two cutting edges of completely different geometry are simultaneously in contact with the workpiece [85] (Figure 43). This is because the distribution of cutting forces resulting from the different cutting edge geometries can have different directions and amplitudes which change with

the tool wear. This can result in significant change of the force pattern captured by a dynamometer (measuring the net force produced by the cutting teeth in engagement with the workpiece). Hence, this leads to difficulties in using the average of peak force values as a measure for wear in cutting edge monitoring.

Shi et al. examined cutting force signals in frequency (FFT) or time-frequency domains (STFT) [85] related to broaching dovetail slots. They observed some differences in patterns with increased tool wear in different segments. However, such approaches that identify changes in the amplitude of particular frequency bands are setup specific (e.g., machine tool, tool design) and therefore, have limited application to other scenarios unless experiments for system characterisation are carried out. Plotting orbital diagrams (Figure 44) [86] of cutting (*Fc*) and push off/radial force (*Fr*) forces, and observing their correlation with the level of tool flank wear (*VB*) has proven an interesting and efficient method to monitor the process. While monitoring peak forces could be a useful technique to detect significant tool malfunctions (e.g., breakage, wear), it might not be sensitive enough to capture small deteriorations such as chipping.

Considering the complexity of interpreting cutting forces in broaching, some researchers have turned to artificial intelligence methods, such as neural networks [6] or support vector machines [86] to detect various tool malfunctions (e.g., wear, chipping and breakage of the cutting edges). In these approaches, the entire signal from a broaching pass is treated as a pattern whose change over time is tracked in the time domain. The literature to date suggests that these artificial intelligence methods appear to be able to handle the complexity in patterns of cutting forces. However, these methods are not without their limitations, particularly as related to the phenomena governing tool failure modes, as well as the necessity of acquiring the quantity of signals needed to make robust decisions.

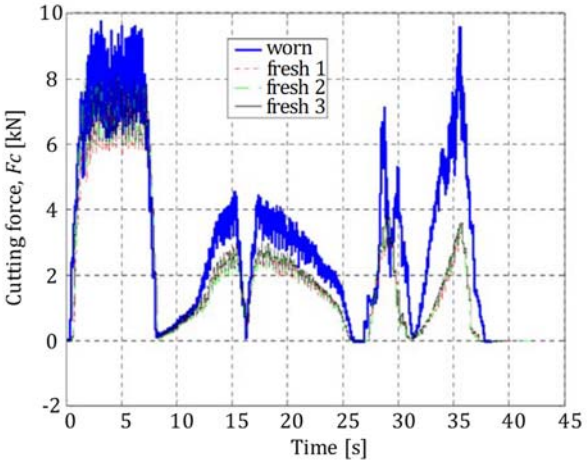


***Figure 43.*** *Cutting force change over time with fresh and worn cutting edges for a dovetail broached slot using an off-the-shelf dynamometer* [85].

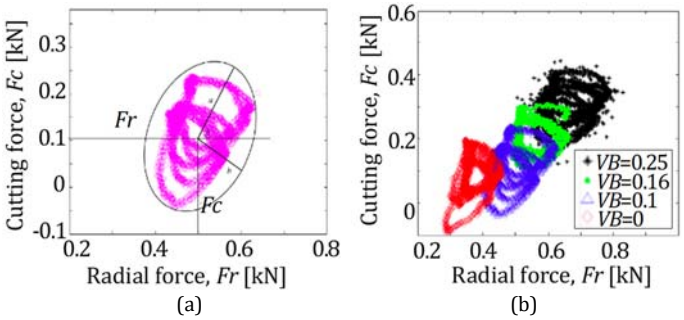


(a) (b)

***Figure 44.*** *Example of an orbital plot of cutting forces at a single level of tool wear (a) and its use to monitor tool wear evolution (b)* [86].

Acceleration and Acoustic Emission (AE) signals have also been used to monitor tool condition [7], in the time, frequency, and time-frequency domains. While these methods have demonstrated their effectiveness in detecting wear and chipping of cutting edges for simple and straight broached profiles, they need to be carefully considered possibly in association with other signals like forces or part displacement, when investigating broached profiles with complex geometry (e.g., fir tree, dovetail).

A novel monitoring setup for broaching was reported by Stoney et al. [92]. This system gauges the sensitivity of the surface acoustic waves based on strain measurements from the workpiece and strain sensors from the simple shaped cutting tools under different cutting conditions. Such integrated strain-based monitoring techniques, equipped with wireless transmission systems (Figure 45), have the advantage over multi-type sensors of being easily implemented in production lines.

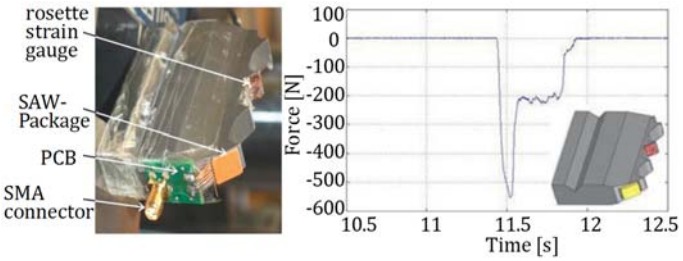


***Figure 45.*** *Strain gauge instrumented broaching tool and output signals* [92].

### *6.2 Workpiece surface monitoring*

Broaching is employed in the manufacture of high-value components (e.g., discs for aeroengines, splines for transmission systems) that sometimes are required to withstand considerable mechanical and/or thermal fatigue, and hence the quality and integrity of the workpiece is of key importance. Since successions of broaching teeth follow the same trajectory, it is very difficult to trace surface imperfections back to a particular cutting edge. The surface generated by one tooth is "wiped" by the following one and so on, until the final "calibration" teeth finish their, theoretical, zero rise per tooth cuts which generate the final workpiece surface. Moreover, since more than two cutting teeth are in contact with the workpiece at any given time, the detection of workpiece defects/anomalies generated by each tooth is even more challenging. For this reason, very few studies are reported in the literature regarding the monitoring of workpiece surface anomalies in broaching.

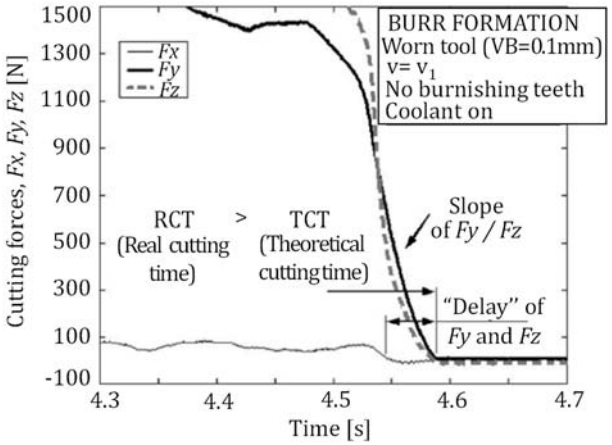


***Figure 46.*** *Burr monitoring* [8].

Surface anomalies at a macro level (e.g., surface deviations from parallelism with the cutting directions, burrs) can be related to cutting forces. As the cutting edges continuously enter and exit the workpiece, the part moves (with magnitudes dependent upon stiffness of the part/machine system) back and forth according to the variation of the cutting forces. This has the potential to generate steps on the workpiece surface [8]. Burrs can be detected by the time delay between the cutting forces in different directions, since the burr is considered as an "additional" cutting length [8] (Figure 46). Axinte et al. [8] also reported that chatter marks could be detected using acceleration signals (components along and normal to the cutting direction) mounted on the machine tool table close to the broached part.

The more challenging aspect, however, is the detection of micro anomalies (e.g., scoring, smearing, plucks, laps) on the workpiece surface during broaching. In this regard, Axinte et al. [4] employed AE together with cutting force signals (sensor fusion) to relate peaks on the AE sensory signals with micro surface anomalies observed when carefully scanning workpiece surfaces (Figure 47).

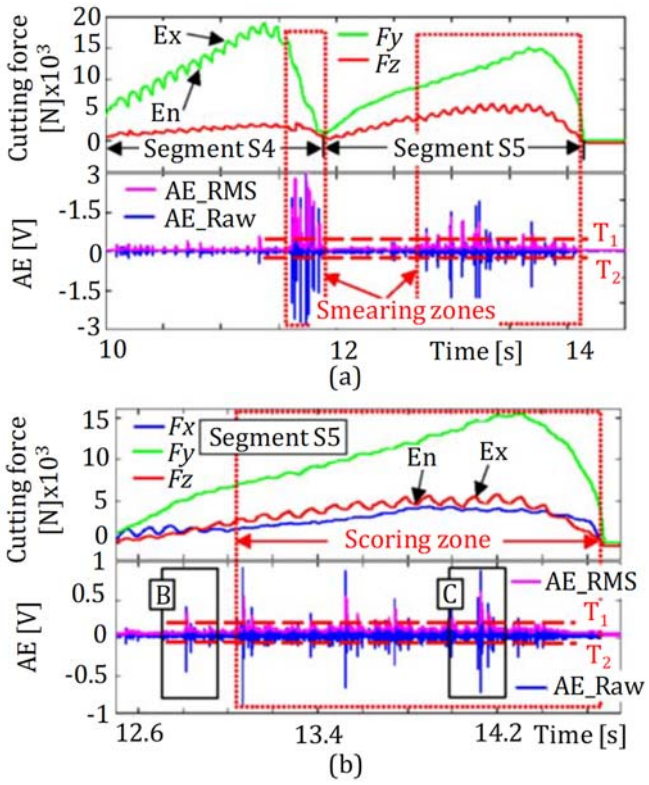


***Figure 47.*** *Identifying surface anomalies by correlating force and AE signals: smearing (a); scoring (b)* [4].

In this work, AE signals were mapped against machined "damage free" surfaces and it was observed that significant AE burst signals (over threshold) occurred only when the teeth entered and exited cutting. The additional AE burst signals that appeared in between could therefore be related to workpiece surface anomalies, on the assumption that tool condition stays the same or its wear status is recognised using the tool condition monitoring techniques described above. Based on this axiom, Axinte at al. [8] were able to identify various micro-level anomalies on the workpiece surface (Figure 48). While some attempts have been made to determine the type of surface anomalies based on the AE frequency analysis, it should be noted that this is dependent on the cutting tool geometry and cutting sequence, and hence might be prone to classification error.

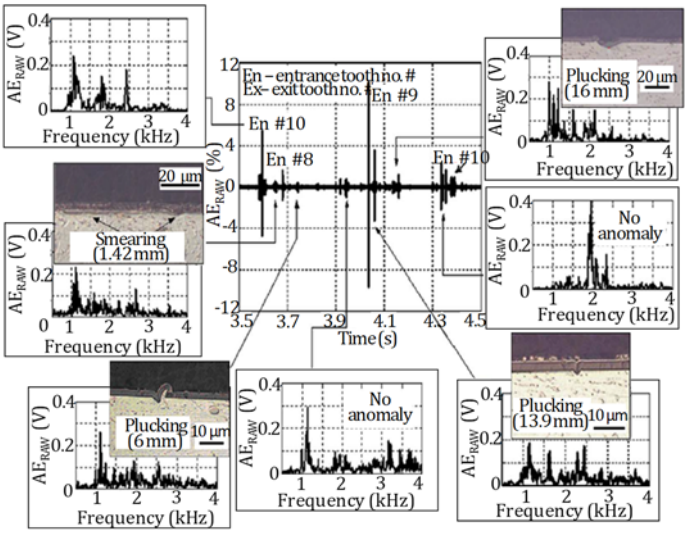


***Figure 48.*** *Correlating AE burst signals with surface anomalies in broaching Ti6Al4V* [8].

Nevertheless, such tests require painstaking attention to detail, as workpiece surface and AE signals need to be carefully scanned in a synchronous manner to establish the correlation between the two. One possible option could be to embed sensors in broaching machine tools, since AE sensors cause little or no disturbance in the machining setup. However, such an approach provides only one dimensional positioning of the anomalies on the workpiece surface, i.e. along the cutting direction. One attempt to overcome this drawback, using a triangulation of three acoustic emission sensors mounted on the workpiece surface, has given a good indication that it is possible to determine the anomalies on the workpiece surface in three dimensional space [9].

A further study [5] uncovered some interesting phenomena of coupled vibrations that led to angled indentation marks on broached complex geometry (e.g., dovetail) slots. This was despite the fact that tools with straight cutting edges were used (Figure 49). These marks are caused when the cutting process transitions between groups of teeth with different geometries (e.g., straight to dovetail) and occurs when the teeth enter and exit the workpiece. These surface anomalies were detected by monitoring the cutting forces and acceleration signals.

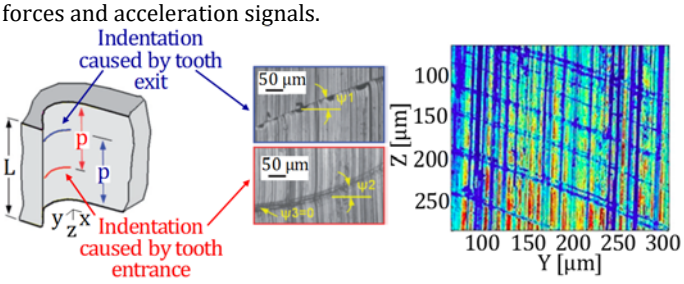


***Figure 49.*** *Angled indentation marks in broaching Ti6Al4V dovetail slots* [5].

## 7. Modelling

Historically, broaching operations were designed based on experience and through trial and error. As more emphasis is placed on productivity and part accuracy, modelling is playing an increasingly important role in the development of broaching technology. End-users are interested in predicting the quality of the broached surface, which requires the consideration and analysis of geometrical accuracy, machining forces, and residual stress. Compared to other cutting processes, such as turning, milling or drilling, there is limited scientific work on the modelling of broaching in the literature. The majority of studies are mainly

focused on the prediction of forces with the objective of verifying the capacity of broaching machines or designing broach stresses. Modelling of residual stress and part accuracy have seldom been treated.

### *7.1 Forces in broaching*

Modelling forces in broaching is challenging due to the complexity of the tool geometry. Macroscopic forces transferred to the broaching tool are the sum of force contributions of several teeth in contact. Moreover, forces vary continuously as teeth enter and exit over time. To simplify the problem, most models developed to date are based on the assumption that a broaching operation can be divided into a sum of orthogonal cutting operations (Figure 50). For instance, Kishawy et al. [37] studied the effect of a single straight cutting edge in contact with the workpiece, oriented perpendicular to the cutting direction. The work material is assumed to flow along a plane perpendicular to the cutting edge (plane strain deformation), thereby dividing a complex cutting edge into several elementary segments. This leads to several limitations, as the model does not consider interactions between sections, especially when cutting edges are curved (e.g., fir tree broaching). Additionally, this approach largely neglects the interaction with the gullet that constrains chip flow as shown by [26] (Figure 51). Nevertheless, such an "orthogonal cutting approach" does obtain a reasonable approximation of forces in broaching.

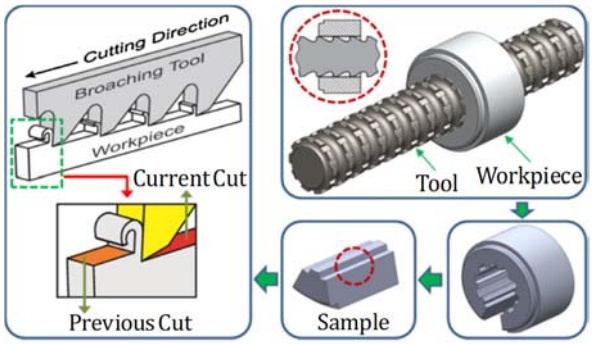


***Figure 50.*** *Principle of broaching modelling based on an orthogonal cutting operation* [37].

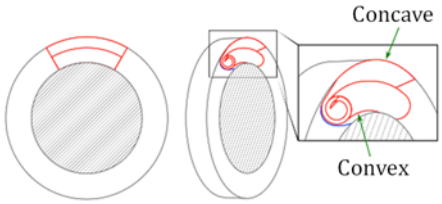


***Figure 51.*** *Interaction between chip formation and gullet in internal broaching* [26].

#### 7.1.1 Empirical modelling

The simplest way to model forces consists of experimentally measuring broaching forces under various cutting conditions (i.e., cutting speed) and cutting tool geometries (i.e., rise per tooth, rake angle, clearance angle) under a defined lubrication condition. An equation is then fitted to the experimental results. This approach has been used by many authors including [27, 30, 60, 65, 70, 73, 99].

Liu et al. [60] developed equations by means of mathematical regression. However, such equations cannot be generalized as they are heavily dependent on the setup, and valid only in the range of operating conditions tested. The majority of authors prefer simple equations, such as (4) and (5) proposed by [27]:

$$F_c = h \cdot a_p \cdot k_{cc} \quad (4)$$

$$F_r = h \cdot a_p \cdot k_{cr} \quad (5)$$

where, $h$ is the rise per tooth, $a_p$ is the width of cut, and $k_{cc}$ & $k_{cr}$ refers to the specific cutting pressure in the cutting and radial directions identified as a result of a surface response depending on cutting speed, rise per tooth, and rake angle (Figure 52).

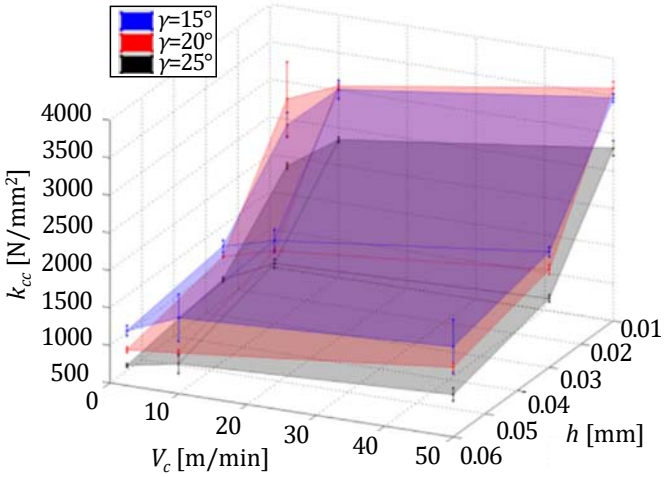


***Figure 52.*** *Surface response of a specific cutting pressure $k_{cc}$* [27].

Vogtel et al. [99] proposed a more complex equation (6):

$$F_c = h^{1-m} \cdot a_p \cdot k_{cc} \quad (6)$$

where, $m$ is a coefficient identified empirically.

Mandrile et al. [65] proposed describing cutting (7) and radial (8) forces based on two terms: a conventional cutting force term that is proportional to the section to be cut ($h \cdot a_p$) and a second term that is independent of the rise per tooth that is linked to the cutting edge sharpness.

$$F_c = h \cdot a_p \cdot k_{cc1} + a_{p.} \cdot k_{cc2} \quad (7)$$

$$F_r = h \cdot a_p \cdot k_{cr1} + a_p \cdot k_{cr2} \quad (8)$$

where, $k_{cc1}$ & $k_{cr1}$ are the specific cutting pressures in the cutting and radial directions respectively, and $k_{cc2}$ & $k_{cr2}$ are the specific coefficients due to the sharpness effect in the cutting and radial directions respectively. $k_{cc1}$, $k_{cr1}$ are identified by a power low equation depending on rise per tooth and rake angle.

Gilormini et al. [30] proposed (9) including an additional term considering the effect of chip evacuation that interacts with the rake face and the gullet. This term increases with the chip length $x$.

$$F_c = h \cdot a_p \cdot (k_{cc} + k'_{cc} \cdot x) \quad (9)$$

where, $k_{cc}$ is the specific cutting pressure, $k'_{cc}$ is the specific chip evacuation coefficient, and $x$ is the chip length.

Empirical orthogonal cutting models are largely accurate for a given application. For this reason, they have been used by some researchers to predict macroscopic resultant forces in broaching case studies. In this vein, Sutherland et al. [93] developed a model to predict macroscopic cutting forces in gear broaching. The model provides a geometrical description of each section to be removed by each set of teeth, and the empirical model estimates the local force. All the local forces active at the same time are then added to determine the resultant macroscopic cutting force at each instant (Figure 53).

Similar approaches to this were presented by Ozlu et al. [73], Vogtel et al. [99], and Ortiz-de-Zarate et al. [71] for fir tree broaching operations, as exemplarily shown in Figure 54 for [71] .

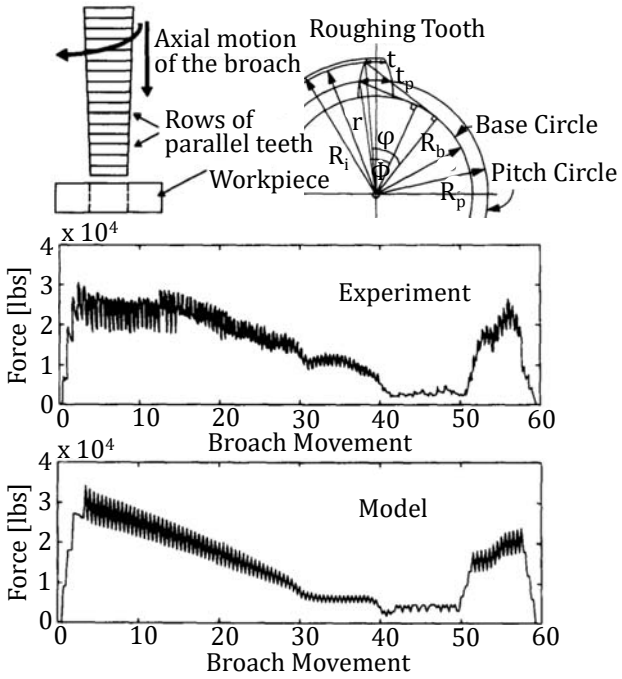


***Figure 53.*** *Cutting force change over time during a gear broaching operation* [93].

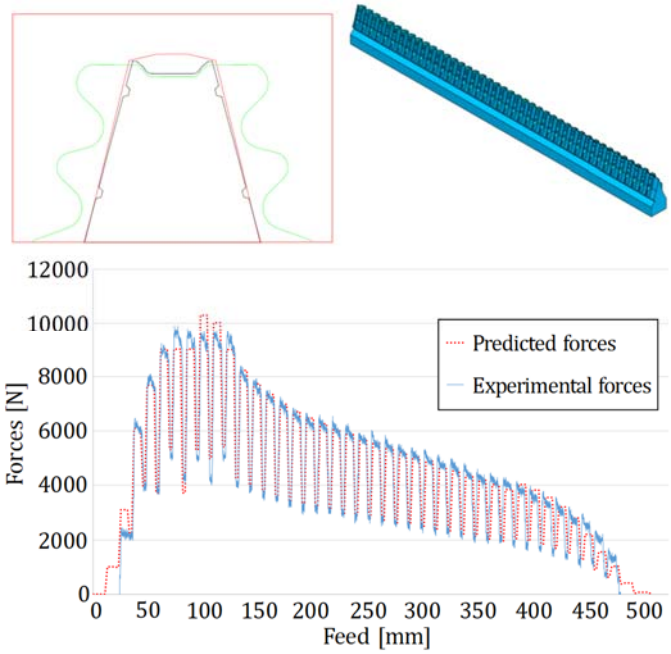


***Figure 54.*** *Cutting force during fir tree broaching* [71].

### 7.1.2 Analytical Modelling

Analytical models deliver a fast response and high degree of accuracy, making them an attractive tool for industrial applications. Some authors, such as Kishawy et al. [37] have developed an analytical model based on the so-called "energy based modelling" with reasonable accuracy. Mandrile et al. [65] also developed force models based on the previous works of Budak et al. [16]. Mandrile applied this model to predict forces during a fir tree broaching operation (Figure 55).

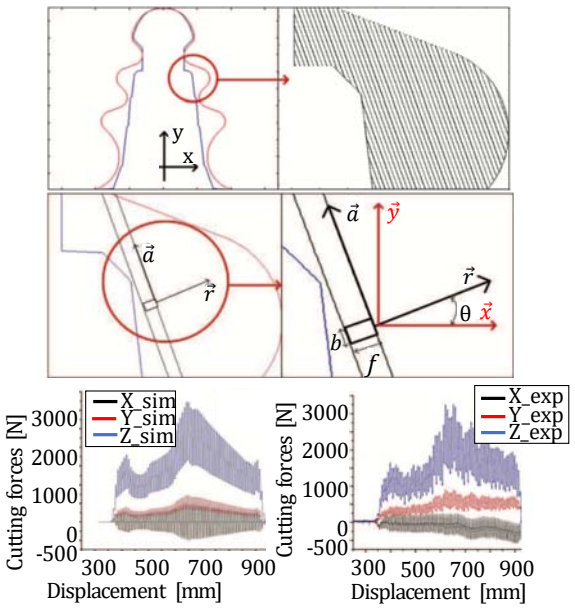


***Figure 55.*** *Changes in cutting forces during fir tree broaching* [65].

### 7.1.3 Finite Element Modelling

Finite Element Modelling (FEM) has gained popularity in recent years, and many authors have applied this method to broaching [27, 55, 63, 70, 100]. The majority of these models however, are derived from prior developments in fundamental orthogonal cutting. Moreover, few works have been found in the literature that consider the low cutting speeds and thin undeformed chip thicknesses typically occurring in broaching.

As chip modeling is a key issue in broaching, many researchers have used a Lagrangian formulation that enables the prediction of chip flow. For instance, Vogtel used the FEM software DEFORM-2D to predict forces and chip morphology for broaching Inconel 718. Kong et al. [55] undertook a similar study with the FEM software ABAQUS Explicit and focused his attention on the serration of chips of a the nickel based alloy GH4169. Nevertheless, both models consider homogeneous materials, which is not realistic when cutting thin chip thicknesses, in which the grain size has the same order of magnitude as the rise per tooth. Thus, Mabrouki et al. [63] developed a Lagrangian model by considering different grain size and different phase ratio (ferrite/pearlite) influences during the broaching of AISI1045 steel. The results revealed the presence of a pseudo-serration due to the shear localisation in the smoothest phase (Figure 56) and could explain the surface roughness problems detailed in Section 2.5 and Figure 16.

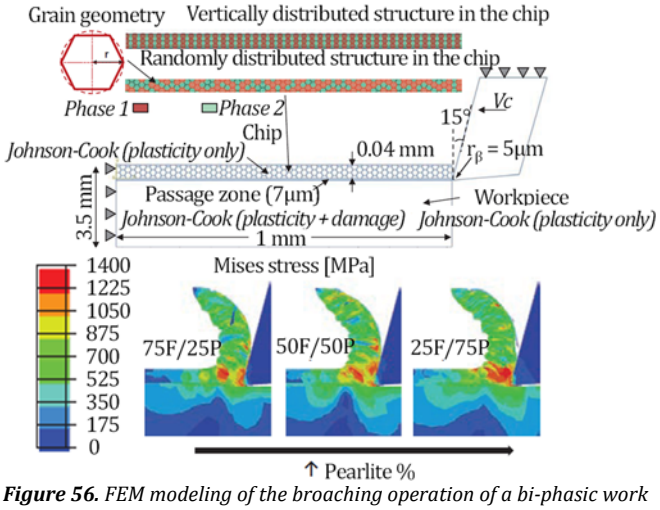


***Figure 56.*** *FEM modeling of the broaching operation of a bi-phasic work material* [63].

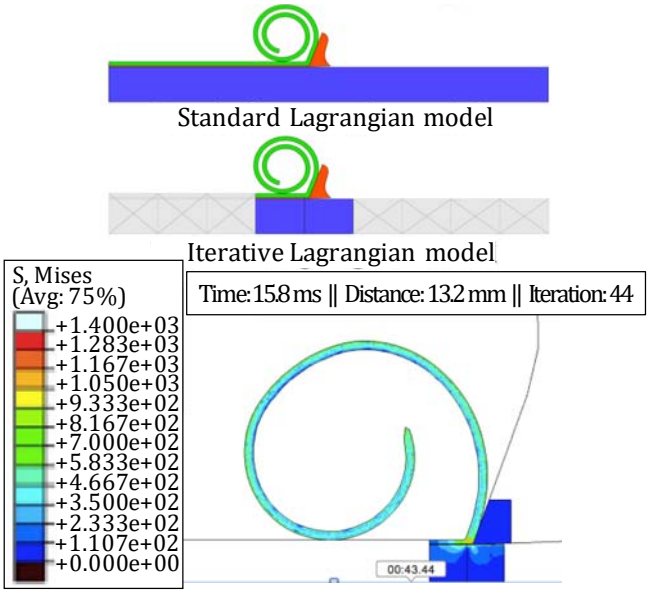


***Figure 57.*** *Interactive Lagrangian modelling of broaching* [27].

The main drawback of the Mabrouki model is the simulated effective cutting duration. The order of magnitude was typically around 0.3 ms due to computation limitations and the chip length was far from being representative of real chips in industrial broaching operations (Figure 56). The effect of chips rolling up was not considered, nor was the interaction between the chip and gullet. To address these shortcomings, Fabre et al. [27] used ABAQUS to develop a so-called IlaM ("Iterative Lagrangian Model") that reduces the number of finite elements and allows for a long duration simulation to predict chips in addition to forces (Figure 57).

### *7.2 Geometric Accuracy*

The broaching process involves very high forces, sometimes resulting in large deflections and dimensional inaccuracies. In an effort to quantify this, some authors have attempted to predict the static deflection of teeth [26, 97] and of parts [26] as discussed in Section 2.10. In addition, as mentioned previously, forces can vary when cutting teeth enter and exit the workpiece, causing the mechanical structure "machine + fixturing + part" to oscillate. During these movements, process parameters such as cutting thickness or rake angle also undergo changes due to the cutting trajectory of the tooth tip [77, 78, 82, 83]. These effects could have an influence on the workpiece accuracy of up to 15%.

### *7.3 Residual stress*

Broaching is a finishing operation on critical surfaces, such as the fir tree of turbine blades, and thus the prediction of the residual stress state is key to controlling fatigue resistance. However, only a few scientific papers have been published on this question, as many works are likely subject to confidentiality agreements. The only work found was that of Schulze et al. [80], dealing with the broaching of an automotive steel AISI5120. The paper focuses on understanding the effects of the final finishing teeth on the residual stress (Figure 58), and reveals a clear interaction between teeth. These results demonstrate the necessity to consider multiple passes to predict the final state of the residual stress (Figure 59), and confirm the findings of similar studies made in finish turning [23, 69].

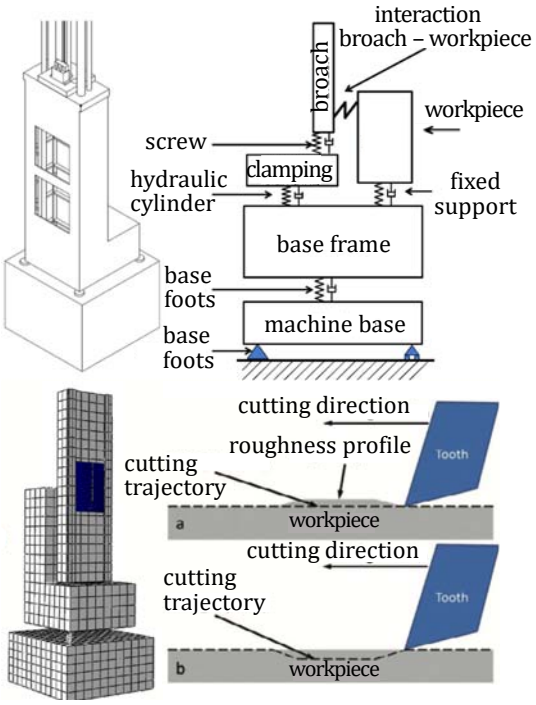


***Figure 58.*** *Modeling of the dynamic response of an entire broaching operation* [83].

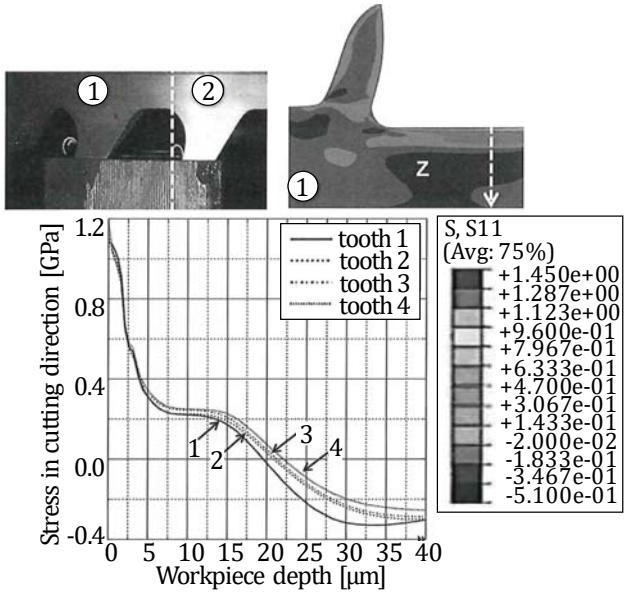


***Figure 59.*** *Residual stress induced by several broaching teeth* [80].

## 8. Industrial applications

The broaching process is typically employed in mass production where the demands for quality and repeatability are high. The process can also be used in low volume production with stringent quality requirements.

Both the automotive and aeronautical sectors make heavy use of broaching processes. In the former, massive production output is commonplace, where for example, more than 5,000 gearboxes are machined and assembled per day in a single plant. Other examples include factories which produce in excess of 10,000,000 wheel hubs per year, or others which manufacture upwards of 5,000,000 brake calipers annually. This can only be done through the use of broaching.

Examples of industrial applications of broaching are set out in the following sections.

*8.1 Automotive*

Crankshaft manufacture involves multiple production processes using complex custom cutting tool solutions. Critical for translating reciprocating linear piston motion into rotation, crankshafts demand the highest possible quality control and tight tolerances. A turn broaching disc solution (Figure 60) can be employed to efficiently turn and broach irregular stock, handling interrupted cuts and impure surfaces. By incorporating various turning cartridges and using standard, thick cemented carbide inserts in cartridges protected by carbide anvils, a custom turn broaching disc can perform a variety of turning and grooving operations, from roughing with interruptions to finishing [84].

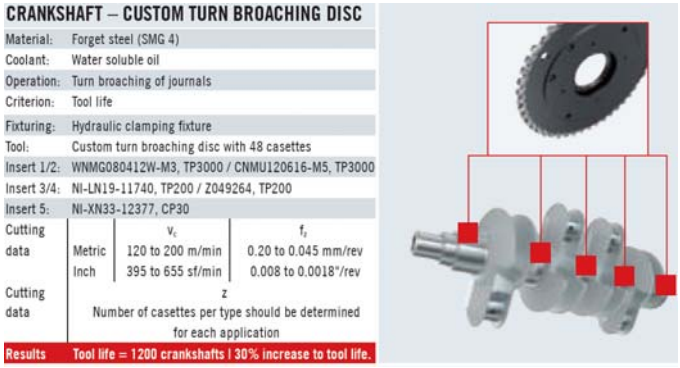

| CRANKSHAFT – CUSTOM TURN BROACHING DISC | | | |
|---|---|---|---|
| Material: | Forget steel (SMG 4) | | |
| Coolant: | Water soluble oil | | |
| Operation: | Turn broaching of journals | | |
| Criterion: | Tool life | | |
| Fixturing: | Hydraulic clamping fixture | | |
| Tool: | Custom turn broaching disc with 48 casettes | | |
| Insert 1/2: | WNMG080412W-M3, TP3000 / CNMU120616-M5, TP3000 | | |
| Insert 3/4: | NI-LN19-11740, TP200 / Z049264, TP200 | | |
| Insert 5: | NI-XN33-12377, CP30 | | |
| Cutting data | | $v_c$ | $f_z$ |
| | Metric | 120 to 200 m/min | 0.20 to 0.045 mm/rev |
| | Inch | 395 to 655 sf/min | 0.008 to 0.0018"/rev |
| Cutting data | z | | |
| | Number of casettes per type should be determined for each application | | |
| Results | Tool life = 1200 crankshafts I 30% increase to tool life. | | |

***Figure 60.*** *Custom turn broaching disc for crankshaft manufacturing* [84].

Another example where an indexable carbide insert broaching tool (Figure 61) is usually employed, is the internal machining of cast iron bearing caps. The system consists of a half-round broach upon which indexable round inserts are mounted. The challenge associated with this application is to produce a large volume of bearing cap components while achieving cycle time reduction and maintaining part accuracy.

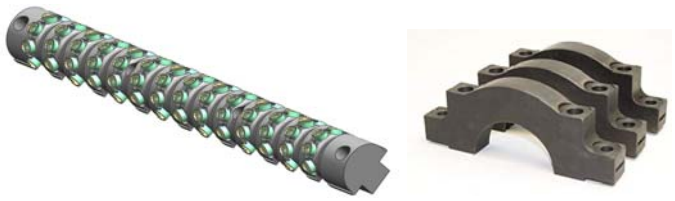

(a) (b)

***Figure 61.*** *Indexable carbide insert broach (a) for internal broaching of bearing cap (b) automotive component* [84].

*8.2 Aeroengine applications*

Broaching is a key technology used in aeroengine component manufacture to produce compressor or turbine blade attachment slots such as dovetail (compressor) or fir tree profiles (turbine) (Figure 62). When broaching nickel-based alloys at low cutting speeds (2-8 m·min$^{-1}$) high-speed-steel is employed while for high cutting speeds (10-20 m·min$^{-1}$) cemented carbide cutting is used (due to increased thermal resistance) (Figure 63) [49, 98].

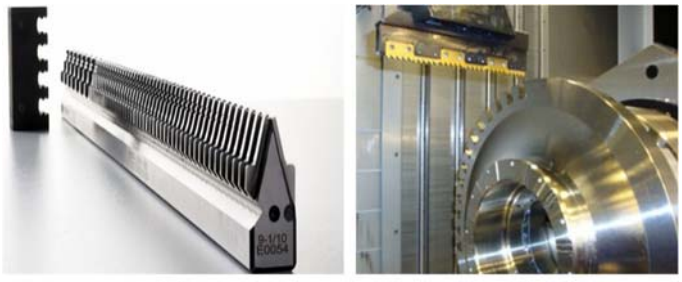

(a) (b)

***Figure 62.*** *(a) Broaching tool for fir tree machining and (b) fir tree of a turbine* [24].

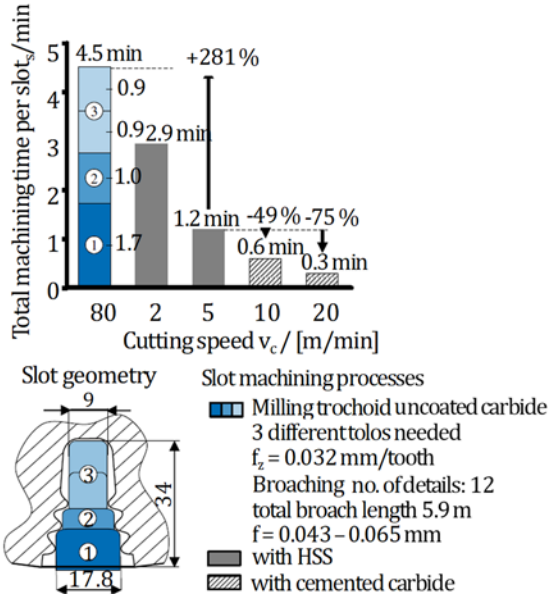


***Figure 63.*** *Comparison of total machining time per slot for pre-slotting with trochoidal milling, broaching with HSS and cemented carbide tools.* [49, 98].

*8.3 Energy/Power generation*

In the field of energy production, broaching is widely used to produce fir tree profiles of gas turbines with similar profiles to those discussed in Section 8.2. In the case of nuclear plants, broaching is the only technique used to produce the shape of the plates located inside the steam generator (Figure 64). The function of these plates is to maintain the tubes containing the water coming from the nuclear reactor (called the "primary loop") whilst simultaneously enabling the flow of the water of the secondary loop around the tubes. Broaching operations are performed with 2 meter-length HSS tools coated with TiN on the flank face, using low cutting speeds (≈3 m·min$^{-1}$) and mineral oil.

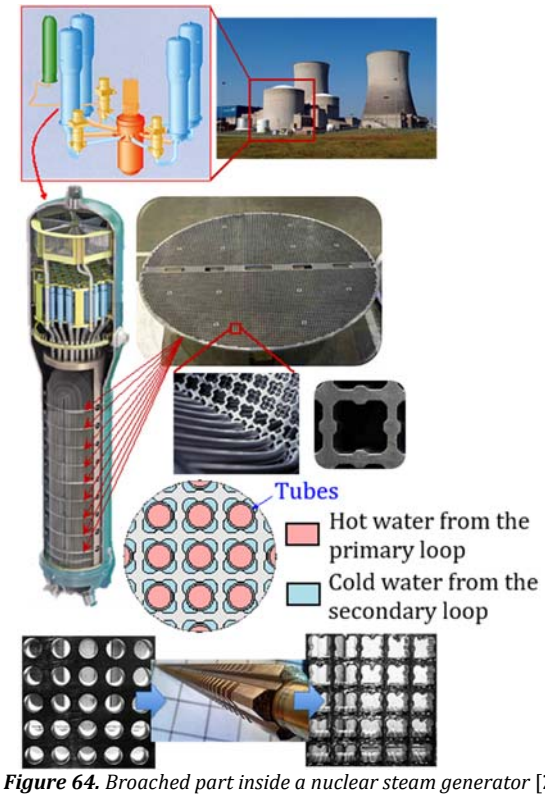


***Figure 64.*** *Broached part inside a nuclear steam generator* [26].

## 9. Alternative Processes

The main disadvantages of the broaching process are the high capital cost and the substantial size and inflexibility of the machine tools. Other drawbacks include costly tooling; lengthy setup, validation and changeover times; high cutting forces (up to 10,000 N); relatively long manufacturing times; and broaching speeds as low as 2 m·min$^{-1}$ required for cutting heat resistant alloys.

Alternative productive processes such as Wire EDM, Milling, Super Abrasive Machining, Electrochemical Machining, Rotary Broaching and Gear skiving are becoming competitive solutions to broaching and are described in more detail below.

### *9.1 Wire Electrical Discharge Machining (WEDM)*

EDM processes are characterized by a purely thermal material removal mechanism which allows the machining of workpieces with virtually no mechanical process forces. High form accuracies can therefore be achieved, including in the case of high strength materials. Limitations of the process are comparatively low productivity and a thermally affected rim zone including inevitable tensile residual stress on the surface. This stress has to be minimized by appropriate trim cut strategies with reduced energies [46].

Welling [103] analyzed the productivity, geometrical accuracy, surface integrity, and bending fatigue strength of WEDM produced parts, compared to broaching and grinding when machining 40 mm high fir tree profiles in Inconel 718. For a given surface roughness requirement of *Ra* < 0.8 µm, in WEDM one main and two trim cuts were necessary resulting in overall average cutting rates of 40-80 mm$^2$·min$^{-1}$ and a form accuracy better than ± 5 µm, [51, 103] (Figure 65). All surfaces featured a small thermally affected rim zone including a thin white layer, a heat affected layer, and a tensile residual stress zone. The overall thickness of the thermally affected layer was less than the thermo-mechanically affected rim zone observed in the broaching and grinding samples. When a worn broaching tool was utilised tensile residual stress was also observed, while compressive stress was identified in the ground samples.

High Cycle Fatigue Bending tests (HCFB) showed failure moments of the same magnitude for both the broached and WEDM manufactured specimens, which suggests that the surface integrities were comparable from a technological and part functionality point of view [102] ( Figure 66). Additional low cycle tensile-compression tests under industrial conditions revealed similar results [103]. Further finishing of the EDM parts by shot [101] and hammer peening [96] could even increase fatigue strength. Advanced process monitoring of EDM signals for quality assurance of the surface integrity is under development [50] and more specifically, concepts for a digital twin of the WEDM produced components are planned in the near future [33]. The productivity of this process amounts to only 10% of broaching, but the investment costs are also in the range of 10% [103]. This solution has the additional advantage of production reliability.

Relying on one broaching machine means that production comes to a complete stop if the machine is down for maintenance or repair, which is not the case in a multiple-unit WEDM system. Therefore, when analysing the machining of a single profile slot, reduced operating costs and higher flexibility is achieved with WEDM (Figure 67). An additional advantage of WEDM is that it is possible to quickly change to a new cutting shape, whereas broaching requires, in most instances, between 9 months to a year to develop a completely new tool.

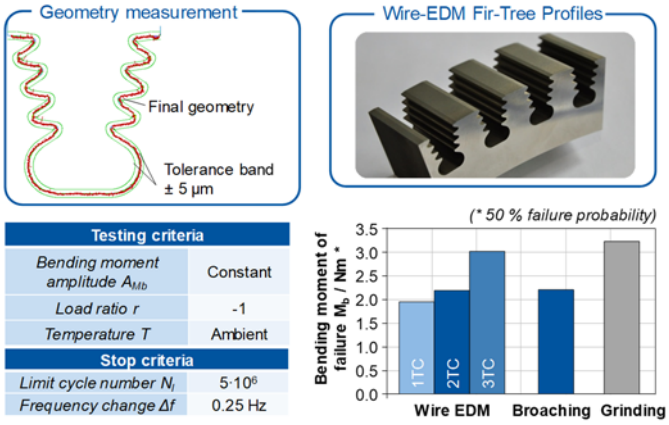


***Figure 65.*** *Geometrical accuracy in WEDM of fir tree profiles and bending fatigue strength of Inconel718 as a function of the applied strategy (number of trim cuts TC) in comparison to broaching and grinding.* [38, 102].

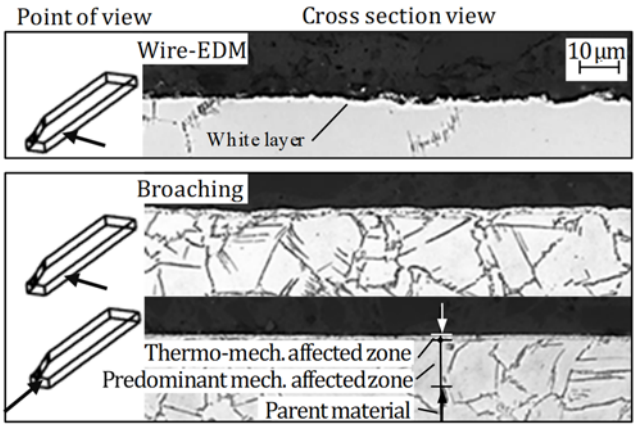


***Figure 66.*** *Surface integrity analysis for WEDM and Broaching, based on* [102].

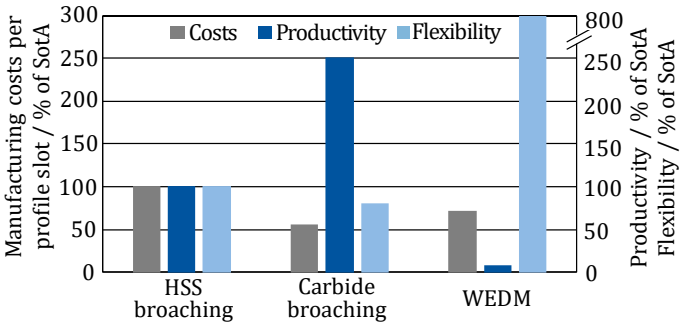


***Figure 67.*** *Cost comparison of carbide broaching and WEDM compared to HSS broaching when machining fir tree profiles* [15].

### *9.2 Milling*

A second alternative to broaching is milling. Klocke et al. [48] studied the potential of manufacturing fir trees by milling and carried out milling tests in Allvac 718 Plus and Inconel 718 using carbide and ceramic mills. They observed that considering surface integrity and metrological accuracy, milling is a viable alternative to broaching to increase flexibility when producing fir tree slots.

In a further development, Iruba [35] together with the companies Delcam and Hermle, were able to create complex fir tree profiles with a C60 five-axis strategy called trochoidal machining (Figure 68).

***Figure 68.*** *Fir tree milling* [35].

*9.3 Super Abrasive Machining (SAM)*

Aspinwall et al. [3] analysed the finishing of a fir tree root form with a single layer/electroplated CBN (B46, B76 and B91) and diamond (D46) grinding wheels, when cutting Udimet 720 using an oil based fluid in a down grinding mode on single sided specimens. They observed that tool wear was lower for CBN grit compared to diamond grit. However, workpiece roughness was lower with $R_a$ approaching 0.75 µm when using D46 wheels. It would appear that the higher rotational speed produced lower grinding wheel wear. No workpiece burning was observed irrespective of grit type under the tested conditions.

In the work of Gonzalez et al. [31] superabrasive machining of Inconel 718 slots were compared to flank milling in conventional machining centers. They found that flank SAM presented lower values for surface roughness than flank milling. In the cross-sectional analysis , it was observed that the conventional technique generated irregularities on the machined surface. The reason why such surface irregularities were eliminated using flank SAM is because the wear rate of the grinding tools was more uniform, resulting in a more even surface finish. It is also worth noting that no white layer was observed in any case. The study also highlighted that compressive residual stress and tensile residual stress increased on the machined surface by flank SAM and flank milling respectively, producing values five times higher than the conventional technique. Microhardness also presented higher values on the flank SAM surface as a direct product of compressive residual stresses. These results indicate that flank SAM techniques can be considered as an alternative to roughing strategies for difficult to cut materials.

*9.4 Electrochemical Machining (ECM)*

ECM processes are characterized by a purely chemical material removal mechanism, which allows the machining of workpieces without any thermo-mechanical rim zone formation and independent of physical material properties. High material removal rates can generally be achieved based on the real machining principle, and virtually no tool wear occurs. Drawbacks of the process include cost intensive initial efforts necessary to design the complete tooling system, as no equidistant working gap is developed along the electrolyte flow path. The process therefore is generally inflexible and only suitable for (large) serial production [46].

A tool cathode for Sinking ECM with a frontal active area and the principle of Wire ECM for machining fir tree profiles is shown in Figure 69. Although the former process is used in industry, no detailed scientific publications are available to date. However, the successful application of Wire ECM in macro geometries with improved flushing conditions has been the subject of study.

Bergs et al. [14] published achievable material removal rates for Sinking ECM roughing of fir tree profiles in a powder-based nickel super alloy in the order of magnitude of 900 $mm^3 \cdot min^{-1}$ with feed rates of up to 3.5 $mm \cdot min^{-1}$. The estimated geometrical accuracy after finishing was typically in the range of ± 10-20 µm. In a final economic analysis, they observed that the machining time per slot was 20% higher than the state of the art (Broaching-HSS), but the costs were 25% lower. This is because final operating costs are lower in the given scenario of serial production.

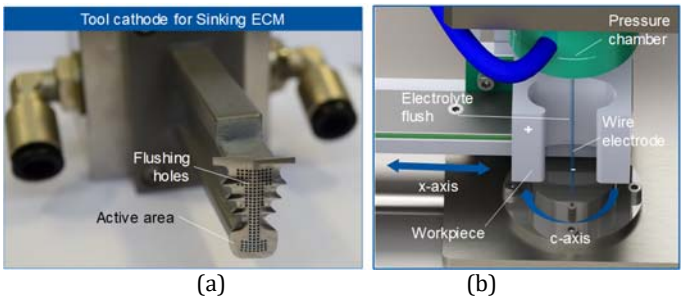


(a) (b)

***Figure 69.*** *ECM and Wire ECM – tool cathode for sinking ECM (a) and principle of Wire ECM with rotating tool electrode (b),* [14, 45].

Klocke et al. [44] evaluated the Wire ECM process with rotating tool electrodes and additional flushing when machining 40 mm high nickel-based workpieces. Cutting rates up to 20 $mm^2 \cdot min^{-1}$ and resulting form accuracies in the range of ± 30 µm were observed for prototype machine tool concepts, with only 20-40% of resulting operating costs compared to EDM [45]. This also could prove an interesting technique for industrial application.

*9.5 Rotary broaching*

Rotary broaching [87] is a rapid machining method that cuts shapes into (i.e., internal cutting) or outside (i.e., external cutting) a workpiece. It involves using a broach, which is ground to the desired finished form, and a rotary broaching tool holder on a lathe, mill, or other CNC machine. The rotary broaching tool holder has a free-rotating spindle on the front end, which holds the broach at a 1 degree angle (Figure 70a). The broach is driven by the workpiece, so no live tooling is needed. In a lathe, upon contact with the workpiece, the broach and tool holder spindle will begin to rotate 1:1 with the workpiece while the body of the tool holder is held stationary (Figure 70b). In a mill, the workpiece is stationary, so the broach and tool holder body rotates in the spindle of the machine (Figure 70c).

The 1 degree angle that is built into the tool holder allows the broach to have only one point of engagement at a time. In this way very little thrust is required from the machine, which makes it possible to perform broaching on virtually any CNC machine.

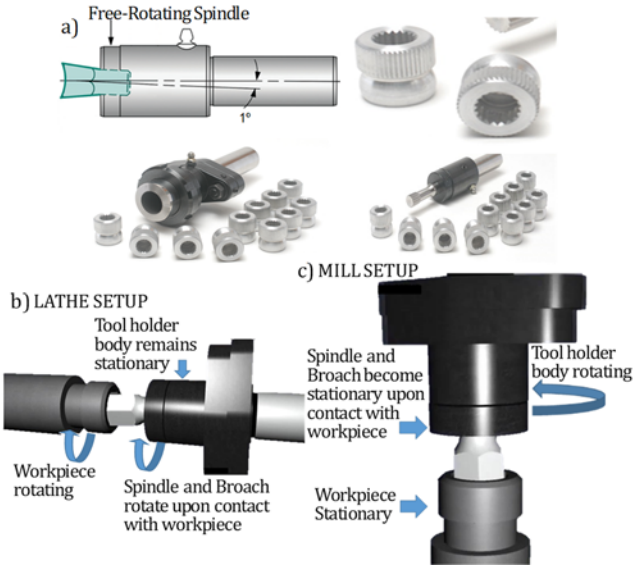


***Figure 70.*** *(a)Tool holder for a rotary broach and some examples of components manufactured by this process, (b) rotary broaching in a lathe and (c) rotary broaching in a mill* [87].

The tool holder should be properly centered to prevent off-centre cutting and its resulting problems. The tool typically has a +0/-.0012 µm tolerance, and usually the internal broaches are manufactured to the upper limit of the required workpiece tolerance to maximize tool life, e.g. if the major diameter (outer diameter) of a serration needs to be between .513-.517, the tool is manufactured to the "high limit" of .517.

Rotary broaching is less expensive than step broaching and no special broaching machine is required, maintaining similar cycle times (5-10 seconds) and tolerances .0012 µm.

*9.6 Gear skiving*

Broaching can be used in large scale production of internal gears. It is also possible to machine external gears by broaching but this is rather uncommon, as processes like gear hobbing are more productive and flexible. Also, broaching is limited, as the process kinematics and tool shape impede manufacturing of internal or external gears with nearby geometrical interference. Thus, modern gearing applications profit from gears integrated into more complex parts like the shaft or case, which can not more manufactured by broaching.

Gear skiving (Figure 71) is applicable to internal as well as external gears and the geometrical workpiece quality can be improved by adapting the process kinematics. Based on its high level of development and high flexibility, gear shaping is used for internal gears in smaller batch sizes and external gears with nearby interference contour. On the downside gear shaping is characterized by low productivity. Gear skiving offers a high potential to improve runtimes with simultaneously high flexibility. Therefore, it competes with gear shaping as well as broaching and is increasingly being used in industrial production of internal gears [88].

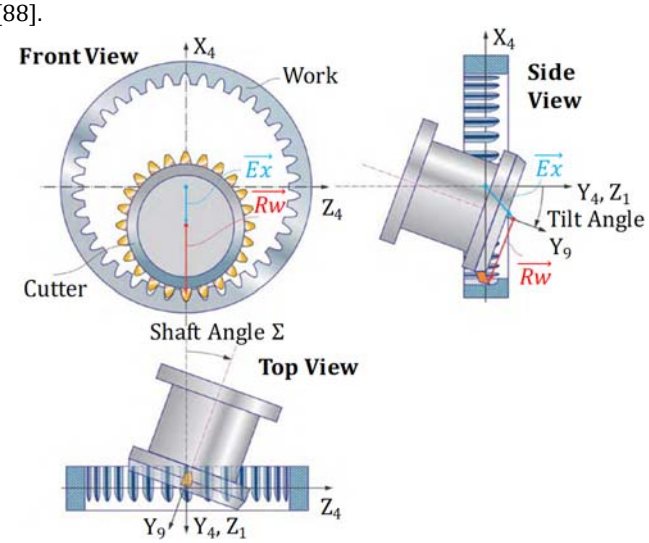


***Figure 71.*** *Basic geometry and kinematics of gear skiving* [88].

## 10. Future trends

The most relevant trends to consider for the future are the following:

- Hard broaching: The technical requirements of broaching are becoming increasingly demanding. Clearances in the assemblies of broached pieces are being reduced in order to improve their efficiency (for example less noise and more efficient gearboxes, etc.). Thus, in many cases the dimensional and geometric tolerances and roughness specifications require that the broaching process need to be carried out after the heat treatment of the workpiece. Re-broaching operations in hardened workpieces is becoming more common and the part qualities achieved are very similar to grinding.
- Coolant: Dry broaching [39] is becoming more common due to environmental requirements. This approach presents the following advantages:
  - Eliminating the use of coolant and thus reducing consumption and waste of water and cutting oils.
  - Components come out clean from the machine (no need for subsequent washing machines).
  - Production lines are cleaner.
  - The condition of the broaching machine is improved by avoiding aggressive liquids that may damage the machine components.
- Cutting tools: The use of powder-metallurgy for both HSS and cemented carbides with improved coatings is increasing.
- Process Monitoring:
  - Machines could be equipped with load cells, and power monitoring sensors installed on the drives, to enable tool condition monitoring and thus, ensure component quality. Also, adequate CNC signals (e.g., servo motor data) can be directly used for this purpose.
  - Temperatures of drives and slides are also being measured to gain information about process conditions.
  - Monitoring the vibrations in components and subassemblies is also an area for future study, as broaching machines generate vibrations due to the intermittent nature of the cutting operation, as well as the interactions between the machine and process dynamics.

## 11. Implications for academia

This paper has highlighted several potential aspects for further study, namely:

- Empirical and modelling studies (as discussed in Section 7), considering the influence of input variables, such as cutting speed.
- Multiscale and multiphase simulations integrating physical base material and friction models, among other phenomena, help gain an understanding of the impact of the broaching process on fundamental variables (forces and temperatures), or industrial outcomes (roughness, residual stress, material damage and burrs).
- With the understanding of the distribution of cutting forces, there is an opportunity to propose new broaching geometries (e.g., succession of cuts, chip thickness gradients) to better distribute the cutting forces for the reduction of the machine tool deflections, and hence improve part quality.
- Process monitoring with multi-sensors and data fusion, to ensure component quality and obtain data driven models.

## 12. Conclusions

The following conclusions can be drawn from this review:

- Although the broaching process has some fundamental shortcomings (such as high initial investment costs; costly consumables; lack of versatility; lengthy setup, validation and changeover times; high cutting forces; and quite long manufacturing times) it is still among the most effective machining processes for demanding industrial sectors, such as the automotive, aeronautics, and energy industries. This is because the process enables the manufacturing of components with geometric complexity, while delivering high dimensional accuracy (IT6/IT7), good surface finish ($Ra$ = 0.8 µm), and good repeatability. Although competing machining operations, such as wire EDM and milling, are making their presence felt in the market, they are still a long way from replicating the capacity of the broaching process achieved in certain applications.

- Even though several research studies have been published, increasing scientific understanding of the broaching process and developing models for the cutting forces, roughness, etc., there still remains a need to:
  - analyse the influence of some potential key input parameters in fundamental variables and industrial outcomes, and
  - improve existing models to enable their effective, practical, and reliable application in industrial settings.

## Acknowledgements

The authors would like to thank Andreas Klink, Martin Seimann, Thomas Bergs from WZL, RWTH Aachen University, Guillermo Celaya from Ekin, Johan L Eriksson from Seco Tools AB, Iñaki Arrieta, Gorka Ortiz de Zarate, Endika Jimenez de Aberasturi and Aitor Madariaga from Mondragon University, Dorian Fabre from ENISE and Hossam Kishawy from Ontario Tech University.

## References

[1] Ahmad, R., Al-Rawashdeh, H., Hasan, A.O., 2019, Optimization of keyway broach design, Journal of Failure Analysis and Prevention, 19/ 3: 688–697.

[2] Arrieta, I., Courbon, C., Cabanettes, F., Arrazola, P.J., Rech, J., 2017, Influence of the ferritic-pearlitic steel microstructure on surface roughness in broaching of automotive steels, AIP Conference Proceedings, 1896/ 1.

[3] Aspinwall, D.K., Soo, S.L., Curtis, D.T., Mantle, A.L., 2007, Profiled superabrasive grinding wheels for the machining of a nickel based superalloy, CIRP Annals, 56/ 1: 335–338.

[4] Axinte, D., Boud, F., Penny, J., Gindy, N., Williams, D.J., 2005, Broaching of Ti-6-4-Detection of workpiece surface anomalies on dovetail slots through process monitoring, CIRP Annals, 54/ 1: 87–90.

[5] Axinte, D.A., 2007, An experimental analysis of damped coupled vibrations in broaching, International Journal of Machine Tools and Manufacture, 47/ 14: 2182–2188.

[6] Axinte, D.A., 2006, Approach into the use of probabilistic neural networks for automated classification of tool malfunctions in broaching, International Journal of Machine Tools and Manufacture, 46/ 12–13: 1445–1448.

[7] Axinte, D.A., Gindy, N., 2003, Tool condition monitoring in broaching, Wear, 254/ 3–4: 370–382.

[8] Axinte, D.A., Gindy, N., Fox, K., Unanue, I., 2004, Process monitoring to assist the workpiece surface quality in machining, International Journal of Machine Tools and Manufacture, 44/ 10: 1091–1108.

[9] Axinte, D.A., Natarajan, D.R., Gindy, N.N., 2005, An approach to use an array of three acoustic emission sensors to locate uneven events in machining - Part 1: method and validation, International Journal of Machine Tools and Manufacture, 45/ 14: 1605–1613.

[10] Bediaga, I., Ramirez, C., Huerta, K., Krella, C., Munoa, J., 2016, In-process tool wear monitoring in internal broaching, .

[11] Bejnoud, F., Zanger, F., Schulze, V., 2015, Component distortion due to a broaching process, Applied Mechanics and Materials, 794: 239–246.

[12] Bellais, C., 1998, B*rocheuses. Techniques de l'ingenieur - Outillage et machine-outil pour le travail des materiaux, base documentaire*.

[13] Belov, V.S., 1976, Disturbances caused by the cutting force in broaching, Stanki I instrument, 47/ 2: 18–19.

[14] Bergs, T., Smeets, G., Gmelin, T., Heidemanns, L., Harst, S., Klink, A., 2019, ECM roughing of profiled grooves in nickel-based alloys for turbomachinery applications. 19th Machining Innovations Conference for Aerospace Industry.

[15] Bergs, T., Smeets, G., Seimann, M., Doebbeler, B., Klink, A., Klocke, F., 2018, Surface integrity and economical assessment of alternative manufactured profiled grooves in a nickel-based alloy, Procedia Manufacturing, 18: 112–119.

[16] Budak, E., Altintaş, Y., Armarego, E.J.A., 1996, Prediction of milling force coefficients from orthogonal cutting data, Journal of Manufacturing Science and Engineering, 118/ 2: 216–224.

[17] Burnett, M.E., 2016, Improved broaching steel technology, Gear Technology, 44–49.

[18] Chamanfar, A., Monajati, H., Rosenbaum, A., Jahazi, M., Bonakdar, A., Morin, E., 2017, Microstructure and mechanical properties of surface and subsurface layers in broached and shot-peened Inconel-718 gas turbine disc fir-trees, Materials Characterization, 132: 53–68.

[19] Chapman, W., 1999, Modern machine shop handbook for the metalworking industries.

[20] Chen, Z., Colliander, M.H., Sundell, G., Peng, R.L., Zhou, J., Johansson, S., Moverare, J., 2017, Nano-scale characterization of white layer in broached Inconel 718, Materials Science and Engineering: A, 684: 373–384.

[21] Chen, Z., Moverare, J.J., Peng, R.L., Johansson, S., Gustafsson, D., 2016, On the conjoint influence of broaching and heat treatment on bending fatigue behavior of Inconel 718, Materials Science and Engineering: A, 671: 158–169.

[22] Denkena, B., Biermann, D., 2014, Cutting edge geometries, CIRP Annals, 63/ 2: 631–653.

[23] Dumas, M., Valiorgue, F., Van Robaeys, A., Rech, J., 2018, Interaction between a roughing and a finishing operation on the final surface integrity in turning, Procedia CIRP, 71: 396–400.

[24] Ekin [online], *http://www.ekin.es*.

[25] Enache, S., Belousov, V., 1983, *Proiectarea sculelor aschietoare*.

[26] Fabre, D., 2016, *Mécanismes de coupe induits par le brochage d ' un acier inoxydable ferrito-martensitique*.

[27] Fabre, D., Bonnet, C., Rech, J., Mabrouki, T., 2017, Optimization of surface roughness in broaching, CIRP Journal of Manufacturing Science and Technology, 18: 115–127.

[28] Federal broach & machine company [online], https://federalbroach.com/flat_broaches.php.

[29] Forst, O., 2000, Forst manual [online], *www.forst-online.de*.

[30] Gilormini, P., Felder, E., Tronchet, L., Leroy, F., Le Maitre, F., 1984, A comparative analysis of three machining processes: broaching, tapping and slotting, CIRP Annals, 33/ 1: 19–22.

[31] González, H., Pereira, O., Fernández-Valdivielso, A., López de Lacalle, L.N., Calleja, A., 2018, Comparison of flank super abrasive machining vs. Flank milling on Inconel® 718 surfaces, Materials, 11/ 9: 1638.

[32] Grigoriev, S.N., Cherkasova, N., Filatov, P., Vereschaka, A.A., 2015, Surface modification of broaches from the powder high speed steels applied to processing of aviation products from heat-resistant alloys, Advanced Materials Research, 1064: 142–147.

[33] Holsten, M., Klink, A., Bergs, T., 2019, Concepts for advancing the use of process data in electrical discharge machining, Procedia CIRP, 82: 220–223.

[34] Hosseini, A., Kishawy, H.A., 2013, On the optimized design of broaching tools, Manufacturing science and engineering, 136/ 1.

[35] Iruba [online], *https://www.iruba.de/*.

[36] Jones, F.D., Hamilton, D.T., Lucas, C.L., 1914, Broaching. The industrial press.

[37] Kishawy, H.A., Hosseini, A., Moetakef-Imani, B., Astakhov, V.P., 2012, An energy based analysis of broaching operation: Cutting forces and resultant surface integrity, CIRP Annals, 61/ 1: 107–110.

[38] Klink, A., 2016, Process signatures of EDM and ECM processes - Overview from part functionality and surface modification point of view, Procedia CIRP, 42: 240–245.

[39] Klocke, F., Döbbeler, B., Seimann, M., 2016, Dry broaching using carbon free steel as tool material, Procedia CIRP, 46: 496–499.

[40] Klocke, F., Doebbeler, B., Seimann, M., Binder, M., 2016, Towards high productive roughing of profiled grooves in nickel based alloys. ASME Turbo Expo 2016.

[41] Klocke, F., Gierlings, S., Brockmann, M., Veselovac, D., 2014, Force-based temperature modeling for surface integrity prediction in broaching nickel-based alloys, Procedia CIRP, 13: 314–319.

[42] Klocke, F., Gierlings, S., Brockmann, M., Veselovac, D., 2012, Influence of Temperature on Surface Integrity for Typical Machining Processes in Aero Engine Manufacture, Procedia Engineering, 19: 203–208.

[43] Klocke, F., Gierlings, S., Veselovac, D., 2012, Concept for temperature control in broaching nickel-based alloys, Key Engineering Materials, 523: 469–474.

[44] Klocke, F., Herrig, T., Klink, A., 2018, Evaluation of wire electrochemical machining with rotating electrode for the manufacture of fir tree slots, ASME Turbo Expo 2018.

[45] Klocke, F., Herrig, T., Zeis, M., Klink, A., 2018, Experimental investigations of cutting rates and surface integrity in wire electrochemical machining with rotating electrode, Procedia CIRP, 68: 725–730.

[46] Klocke, F., Klink, A., Veselovac, D., Aspinwall, D.K., Soo, S.L., Schmidt, M., Schilp, J., Levy, G., Kruth, J.P., 2014, Turbomachinery component manufacture by application of electrochemical, electro-physical and photonic processes, CIRP Annals, 63/ 2: 703–726.

[47] Klocke, F., Kuchle, A., 2011, Manufacturing Process 1. Springer.

[48] Klocke, F., Seimann, M., Binder, M., Doebbeler, B., 2018, Milling of fir-tree slots in allvac 718 plus, Procedia CIRP, 77: 409–412.

[49] Klocke, F., Vogtel, P., Gierlings, S., Lung, D., Veselovac, D., 2013, Broaching of Inconel 718 with cemented carbide, Production Engineering, 7/ 6: 593–600.

[50] Klocke, F., Welling, D., Klink, A., Perez, R., 2014, Quality assessment through in-process monitoring of wire-EDM for fir tree slot production, Procedia CIRP, 24: 97–102.

[51] Klocke, F., Welling, D., Klink, A., Veselovac, D., Nöthe, T., Perez, R., 2014, Evaluation of advanced Wire-EDM capabilities for the manufacture of fir tree slots in inconel 718, Procedia CIRP, 14: 430–435.

[52] Komanduri, R., Hou, Z.B., 2000, Thermal modeling of the metal cutting process: Part I—Temperature rise distribution due to shear plane heat source, International Journal of Mechanical Sciences, 42/ 9: 1715–1752.

[53] Komanduri, R., Hou, Z.B., 2001, Thermal modeling of the metal cutting process - Part II: Temperature rise distribution due to frictional heat source at the tool-chip interface, International Journal of Mechanical Sciences, 43/ 1: 57–88.

[54] Komanduri, R., Hou, Z.B., 2001, Thermal modeling of the metal cutting process - Part III: Temperature rise distribution due to the combined

effects of shear plane heat source and the tool-chip interface frictional heat source, International Journal of Mechanical Sciences, 43/ 1: 89–107.
[55] Kong, X., Li, B., Jin, Z., Geng, W., 2011, Broaching performance of superalloy GH4169 based on FEM, Journal of Materials Science and Technology, 27/ 12: 1178–1184.
[56] Kuljanic, E., 1975, Cutting force and surface roughness in broaching, Ann. CIRP, 24/ 1: 77–82.
[57] Kuzin, V., Gurin, V., Shein, A., Kochetkova, A., Mikhailova, M., 2018, The influence of duplex vacuum-plasma treatment on the mechanics of complex-profile cutting tool wearing in the production of aircraft engine parts, Mechanics and Industry, 19/ 7: 704.
[58] Lapointe, F.J., 1914, Key seat broaching machine.
[59] Lapointe, F.J., 1920, U.S. Patent No. 1,339,656.
[60] Liu, Z., Wang, C., Chen, M., Ge, C., Li, M., 2014, A coupling response surfaces methodology of multiple constraints (CRSMMC) for parameters optimization of broach tool in broaching of heat-resistant steel X12CrMoWVNb N-10-1-1, International Journal of Advanced Manufacturing Technology, 74/ 9–12: 1719–1732.
[61] Liu, Z.Q., Chen, M., Wang, C.D., An, Q.L., Ge, C.X., Guo, G.Q., 2014, Investigation performance of AlCrN_based coated broaching tool in broaching of gas turbine material X12CrMoWVNbN1011, Advanced Materials Research, 1017: 361–366.
[62] Loizou, J., Tian, W., Robertson, J., Camelio, J., 2015, Automated wear characterization for broaching tools based on machine vision systems, Journal of Manufacturing Systems, 37: 558–563.
[63] Mabrouki, T., Courbon, C., Fabre, D., Arrieta, I., Arrazola, P.J., Rech, J., 2017, Influence of microstructure on chip formation when broaching ferritic-pearlitic steels, Procedia CIRP, 58: 43–48.
[64] Makarov, V.F., Tokarev, D.I., Tyktamishev, V.R., 2008, High speed broaching of hard machining materials, International Journal of Material Forming, 1/1: 547–550.
[65] Mandrile, S., Dessein, G., Denape, J., Paris, J.Y., Cazenave-Laroche, G Vernault, C., 2012, Identification and modelization of cutting phenomena in broaching to understand tool wear, Conference MUGV.
[66] Meier, H., Ninomiya, K., Dornfeld, D., Schulze, V., 2014, Hard broaching of case hardened SAE 5120, Procedia CIRP, 14: 60–65.
[67] Mo, S.P., Axinte, D.A., Hyde, T.H., Gindy, N.N.Z., 2005, An example of selection of the cutting conditions in broaching of heat-resistant alloys based on cutting forces, surface roughness and tool wear, Journal of Materials Processing Technology, 160/ 3: 382–389.
[68] Mondelin, A., Claudin, C., Rech, J., Dumont, F., 2011, Effects of lubrication mode on friction and heat partition coefficients at the tool-work material interface in machining, Tribology Transactions, 54/ 2: 247–255.
[69] Mondelin, A., Valiorgue, F., Rech, J., Coret, M., Feulvarch, E., 2012, Hybrid model for the prediction of residual stresses induced by 15-5PH steel turning, International Journal of Mechanical Sciences, 58/ 1: 69–85.
[70] Ortiz-De-Zarate, G., Madariaga, A., Garay, A., Azpitarte, L., Sacristan, I., Cuesta, M., Arrazola, P.J., 2018, Experimental and FEM analysis of surface integrity when broaching Ti64, Procedia CIRP, 71: 466–471.
[71] Ortiz-de-Zarate, G., Soler, D., Cuesta, M., Madariaga, A., Garay, A., Arrazola, P.J., 2017, Predictive model of forces for aeronautic materials fir tree broaching, Proceeding of ISABE, .
[72] Ozelkan, E.C., Ozturk, O., Budak, E., 2011, Identifying parameters of a broaching design using non-linear optimisation, International Journal of Modelling, Identification and Control, 12/ 3: 244–252.
[73] Ozlu, E., Engin, S., Cook, C., El-Wardany, T., Budak, E., 2010, Simulation of broaching operations for tool design optimization, .
[74] Ozturk, O., Budak, E., 2003, Modeling of broaching process for improved tool design, Proceedings of IMECE'03 2003 ASME, 16–21.
[75] Rech, J., Arrazola, P.J., Claudin, C., Courbon, C., Pusavec, F., Kopac, J., 2013, Characterisation of friction and heat partition coefficients at the tool-work material interface in cutting, CIRP Annals, 62/ 1: 79–82.
[76] Rech, J., Hamdi, H., Valette, S., 2008, Workpiece Surface Integriy, Chapter from Machining Fundamentals and recent Advances.
[77] Schulze, V., Boev, N., Zanger, F., 2012, Numerical investigation of the changing cutting force caused by the effects of process machine interaction while broaching, Procedia CIRP, 4: 140–145.
[78] Schulze, V., Boev, N., Zanger, F., 2012, Simulation of metal cutting process with variable cutting thickness during broaching, Procedia CIRP, 1: 437–442.
[79] Schulze, V., Meier, H., Straussb, T., Gibmeier, J., 2012, High speed broaching of case hardening steel SAE 5120, Procedia CIRP, 1: 431–436.
[80] Schulze, V., Osterried, J., Meier, H., Zanger, F., 2011, Simulation of multiple chip formation when broaching SAE 5120 low alloy steel, Advanced Materials Research, 223: 37–45.
[81] Schulze, V., Osterried, J., Strauß, T., 2011, FE analysis on the influence of sequential cuts on component conditions for different machining strategies, Procedia Engineering, 19: 318–323.
[82] Schulze, V., Zanger, F., Boev, N., 2013, Numerical investigations on changes of the main shear plane while broaching, Procedia CIRP, 8: 246–251.
[83] Schulze, V., Zanger, F., Kraußе, M., Boev, N., 2013, Simulation approach for the prediction of surface deviations caused by process-machine-interaction during broaching, Procedia CIRP, 8: 252–257.
[84] SECO [online]: *https://www.secotools.com/article/88912*.
[85] Shi, D., Axinte, D.A., Gindy, N.N., 2007, Development of an online machining process monitoring system: A case study of the broaching process, International Journal of Advanced Manufacturing Technology, 34/ 1–2: 34–46.
[86] Shi, D., Gindy, N.N., 2007, Tool wear predictive model based on least squares support vector machines, Mechanical Systems and Signal Processing, 21/ 4: 1799–1814.
[87] Slater Tools Inc., 2019, Solving manufacturing problems though rotary broaching.
[88] Stadtfeld, H. J., 2014, Power skiving of cylindrical gears on different machine platforms, Gear Technology, 31/1: 52-62.
[89] Stanescu, I., Tache, V., 1979, *Dispozitive pentru machini unelte: Proiectare si Constructie*.
[90] Star Su [online], *https://www.star-su.com/tool-grinders/broach-grinding/utg-series-broach-grinding-machines/*.
[91] Stephens, A.P., 1873, Improvement in broaching machines.
[92] Stoney, R., Pullen, T., Aldwell, B., Gierlings, S., Brockmann, M., Geraghty, D., Veselovac, D., Klocke, F., Donnell, G.E.O., 2014, Observations of surface acoustic wave strain and resistive strain measurements on broaching tools for process monitoring, Procedia CIRP, 14: 66–71.
[93] Sutherland, J.W., Salisbury, E.J., Hoge, F.W., 1997, A model for the cutting force system in the gear broaching process, International Journal of Machine Tools and Manufacture, 37/ 10: 1409–1421.
[94] Terry, W.R., Cutright, K.W., 1986, Computer aided design of a broaching process, Computers and Industrial Engineering, 11/ 1–4: 576–580.
[95] Think productivity, think HSS [online],: *http://hssforum.com/BroachingEN.pdf*.
[96] Trauth, D., Klocke, F., Welling, D., Terhorst, M., Mattfeld, P., Klink, A., 2016, Investigation of the surface integrity and fatigue strength of Inconel718 after wire EDM and machine hammer peening, International Journal of Material Forming, 9/ 5: 635–651.
[97] Vijayaraghavan, L., R, K., 1986, Dimensional accuracy in internal broaching. 12th AIMTDR Conference, 285–287.
[98] Vogtel, P., Klocke, F., Lung, D., 2014, High performance machining of profiled slots in nickel-based-superalloys, Procedia CIRP, 14: 54–59.
[99] Vogtel, P., Klocke, F., Lung, D., Terzi, S., 2015, Automatic broaching tool design by technological and geometrical optimization, Procedia CIRP, 33: 496–501.
[100] Vogtel, P., Klocke, F., Puls, H., Buchkremer, S., Lung, D., 2013, Modelling of process forces in broaching Inconel 718, Procedia CIRP, 8: 409–414.
[101] Welling, D., 2019, Advancements in EDM – Solutions for the production of turbomachinery components. ICTM-Konferenz.
[102] Welling, D., 2014, Results of surface integrity and fatigue study of wire-EDM compared to broaching and grinding for demanding jet engine components made of Inconel 718, Procedia CIRP, 13: 339–344.
[103] Welling, D., 2015, Wire EDM for the manufacture of fir tree slots in nickel-based alloys for jet engine components, Apprimus Verlag.
[104] Weule, H., Fleischer, J., Neithardt, W., Broos, A., Schmidt-Ewig, J.P., Minx, J., 2005, Structural optimization of machine tools under consideration of their static and dynamic behavior within the workspace, Production Engineering. Research and Development, 12/ 2: 201–204.
[105] Zanger, F., Boev, N., Schulze, V., 2014, Surface quality after broaching with variable cutting thickness, Procedia CIRP, 13: 114–119.